IEEE Access
Multidisciplinary ⋮ Rapid Review ⋮ Open Access Journal

Received July 14, 2019, accepted July 31, 2019, date of publication August 2, 2019, date of current version August 19, 2019.

Digital Object Identifier 10.1109/ACCESS.2019.2932805

Robust Physical Layer Security for Power Domain Non-Orthogonal Multiple Access-Based HetNets and HUDNs: SIC Avoidance at Eavesdroppers

MOSLEM FOROUZESH[1], PAEIZ AZMI[1], (Senior Member, IEEE), NADER MOKARI[1], KAI-KIT WONG[2], AND HOSSEIN PISHRO-NIK[3]

[1]ECE Department, Tarbiat Modares University, Tehrn 14115-111, Iran
[2]Department of Electronic and Electrical Engineering, University College London, London WC1E 7JE, U.K.
[3]Department of Electronic and Electrical Engineering, University of Massachusetts Amherst, Amherst, MA 01003-9292, USA

Corresponding author: Paeiz Azmi (pazmi@modares.ac.ir)

This work was supported in part by EPSRC under Grant EP/M016005/1.

ABSTRACT In this paper, we investigate the physical layer security in downlink of Power Domain Non-Orthogonal Multiple Access (PD-NOMA)-based heterogeneous cellular network (HetNet). In this paper, we assume two categories of users are available: 1) Trusted users and 2) untrusted users (eavesdroppers) at which transparency of users is not clear for the BSs, i.e., they are potential eavesdroppers. Our aim is to maximize the sum secrecy rate of the network. To this end, we formulate joint subcarrier and power allocation optimization problems to increase sum secrecy rate. Moreover, we propose a novel scheme at which the eavesdroppers are prevented from doing Successive Interference Cancellation (SIC), while legitimate users are able to do it. In practical systems, perfectly availability of all eavesdroppers' Channel State Information (CSI) at legitimate transmitters are impractical. Also CSIs of legitimate users may be also imperfect due to the error of channel estimation. Hence, we study two cases of CSI availability: 1) Perfect CSI of nodes (legitimate users and eavesdroppers) are available at the BSs and 2) imperfect CSI of nodes are available at the BSs. Since the proposed optimization problems are non-convex, we adopt the well-known iterative algorithm called Alternative Search Method (ASM). In this algorithm, the optimization problems are converted to two subproblems, power allocation and subcarrier allocation. We solve the power allocation problem by the Successive Convex Approximation approach and solve the subcarrier allocation subproblem, by exploiting the Mesh Adaptive Direct Search algorithm (MADS). Moreover, in order to study the optimality gap of the proposed solution method, we apply the monotonic optimization method. Moreover, we evaluate the proposed scheme for secure massive connectivity in Heterogeneous Ultra Dense Networks (HUDNs). Furthermore, we investigate multiple antennas base stations scenario in this literature. Finally, we numerically compare the proposed scheme with the conventional case at which the eavesdroppers are able to apply SIC. Numerical results highlight that the proposed scheme significantly improves the sum secrecy rate compared with the conventional case.

INDEX TERMS Physical layer security, PD-NOMA, resource allocation, monotonic optimization.

I. INTRODUCTION

A. STATE OF THE ART AND MOTIVATION

The increasing demand of high data rates and multimedia applications and scarcity of radio resources encourage operators, research centers, and vendors to devise new methods and products for providing high data rate services for the next-generation 5G network. International Telecommunication Union (ITU) has categorized 5G services into three categories: 1) Ultra-reliable and low latency communication (URLLC), 2) enhanced mobile broadband (eMBB), and 3) massive machine-type communication (mMTC) [1]. In mMTC, massive number of machine-type devices are connected simultaneously. Services like sensing, monitoring, and tagging which are in this category have two main challenges: 1) Scarcity of radio resources which make the deployment of massive connections very difficult and 2) broadcast nature of

The associate editor coordinating the review of this manuscript and approving it for publication was Fangfei Li.

wireless channels which make the massive connections insecure. Massive connectivity is one the main features of future wireless cellular networks which is suitable for IoT [2] and machine-type communications (MTC) services. In massive device connectivity scenarios, a cellular Base Station (BS) connects to large number of devices (in order of 10^4 to 10^6 per Km^2). To achieve high throughput and spectrum efficiency, Heterogeneous Ultra Dense Networks (HUDNs) is a promising solution at which the number of BSs per Km^2 is very large (about 40-50) [3]. In order to overcome the scarcity of radio resources in this category, a new multiple access method called power domain Non-Orthogonal Multiple Access (PD-NOMA) can be adopted at which users are serviced within a given resource slot (e.g., time/frequency) at different levels of transmit power [4], [5]. In this method, users can remove signals intended for other users which have the worse channel conditions, by employing successive interference cancellation (SIC) [6]–[8]. It is necessary to mention that SIC concept was first proposed by Cover in 1972 [7] which is very useful technique, because it imposes lower complexity than joint decoding techniques [8]. It is worth noting that the PD-NOMA technique has attracted significant attentions in both academia and industry, [9]–[12]. It is necessary to mention that it has been confirmed in theory domain [13] and system-level simulations [14] which PD-NOMA surpasses orthogonal frequency-division multiple access (OFDMA) in different points of view such as device connections and spectrum efficiency. Based on these benefits, PD-NOMA is very appropriate to be employed for meeting the 5G requirements such as massive connectivity [15] which is very vital for mMTC and Internet of Things (IoT). Besides, establishment of security in these networks is a dilemma, because wireless transmission has broadcast nature. Therefore, private information that is exchanged between transmitter and receiver is vulnerable of eavesdropping. During the past years, Physical Layer Security (PLS) as a promising idea, has been widely investigated since Wyner presented his work in the security domain [16]. Furthermore, as IoT is employed in wide domains such as commercial, military, and governmental application, security plays an important role in IoT applications [17]. Due to constraints of energy consumption and limited hard-ware in IoT devices, it is very vulnerable with respect to eavesdropping. PLS owing to low computational complexity attracts a lot of attentions and is becoming a suitable solution for secure communications in IoT [18].

B. RELATED WORKS

In recent years, PLS by employing PD-NOMA has been studied from various perspectives. The related works on this topic can be categorized into two main categories, namely: 1) PLS in PD-NOMA based system with single carrier, 2) PLS in PD-NOMA based system with multiple carriers.

1) PLS IN PD-NOMA BASED SYSTEM WITH SINGLE CARRIER

PLS in PD-NOMA based systems with single carrier have been recently studied from different perspectives in the literature such as, maximizing the sum secrecy rate, studying different transmit antenna selection strategies [19]–[24]. To be specific, PLS in single-input single-output (SISO) systems based on the PD-NOMA technology is investigated in [19], at which its objective is maximizing the sum secrecy rate. Moreover, the authors in [20] derive a closed-form expression for the secrecy outage probability in MISO-NOMA system. Moreover, in [24], the authors study PLS of PD-NOMA in large-scale networks with employing stochastic geometry, in which a new exact expression of the outage secrecy rate is derived for single-antenna and multiple-antenna cases. In these works because of single carrier system models, the subcarrier allocation is not considered.

2) PLS IN PD-NOMA BASED SYSTEM WITH MULTIPLE CARRIERS

PLS in PD-NOMA based systems with multiple carriers have been studied for different networks [25]–[27]. Specifically, the authors in [25] study subcarrier and power allocation in the two-way relay wireless network in the presence of multiple preassigned user pairs, a jammer, and an eavesdropper. Moreover, the authors in [26] consider a system model consists of a full-duplex base station, multiple trusted uplink and downlink users, and multiple untrusted users. The aim of [26] is to address the resource allocation algorithm design for the considered system model based on PD-NOMA.

Additionally, in [3], the authors study PD-NOMA-based HUDNs for massive connectivity in 5G. The cost of active user detection and channel estimation in massive connectivity by employing massive MIMO are evaluated in [28]. The authors in [29], propose an inter-cell interference coordination mechanism in dense small cell networks. Millimeter-Wave PD-NOMA in machine-to-machine (M2M) communications for IoT networks is proposed in [30]. The authors in [31] study dynamic user scheduling and power allocation problem for massive IoT devices based PD-NOMA.

It is worth noting that the aforementioned works do not investigate PLS in PD-NOMA based HetNet and HUDNs. Moreover, in these works, it is assumed that eavesdroppers know the channel ordering and are able to perform SIC. Note that eavesdroppers by doing SIC are able to decrease the sum secrecy rate. Hence, to tackle this issue, we propose a novel scheme such that, we do not allow the eavesdroppers to be able to perform SIC, even if they know the channel ordering.

C. CONTRIBUTION

In the following, we summarize the main contributions of this paper as:

- In this paper, we focus on this aspect of PD-NOMA, ‘‘how to avoid eavesdroppers from doing SIC and when users are able to perform SIC?''. From the information theory point of view, user A can perform SIC whenever user B's received Signal-to-Interference-plus-Noise

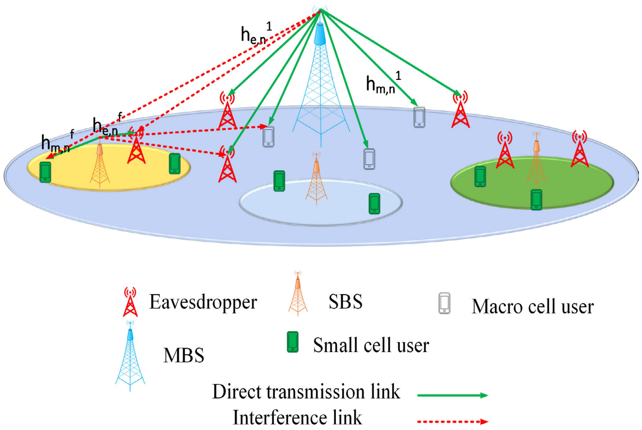

FIGURE 1. Secure transmission in downlink of PD-NOMA based HetNet.

Ratio (SINR) for its signal is less than or equal to user A's received SINR for user B's signal [12], [32], [33]. To this end, we propose a novel resource allocation algorithm such that, we do not allow eavesdroppers to be able to perform SIC, even if they know the channel ordering. In this regard, we formulate an optimization problem at which we introduce a new constraint called SIC avoidance at eavesdropper condition and the main aim is to maximize the sum secrecy rate over transmit power and subcarrier allocation variables.

- In practical systems, perfectly availability of all eavesdroppers' CSI at legitimate transmitters are impractical. Also CSIs of legitimate users may be also imperfect due to the error of channel estimation. Hence, we study two cases of CSI availability, 1) Perfect CSI of nodes (legitimate users and eavesdroppers) are available at the BSs, 2) imperfect CSI of nodes are available at the BSs.
- In addition to the single antenna BSs scenario, we investigate the multiple antennas BSs scenario in the proposed scheme.
- We evaluate the proposed scheme for secure massive connectivity in 5G ultra dense networks. Without loss of generality, for changing our scenario from HetNet to Heterogeneous Ultra Dense Networks (HUDN), we need to extend the dimension of system model. Since the dimension of the optimization problem is very large, proposing a low complex solution is very challenging. To tackle this issue, a new method is proposed at which we consider the uniform transmit power allocation. Moreover, we show the performance of uniform power allocation is close to the performance of our proposed solution.
- We also apply the monotonic optimization method to study the optimality gap of the proposed solution method [34]. For this purpose, we convert the optimization problems to the canonical form of monotonic optimization problem and finally, by exploiting the polyblock algorithm, we solve the monotonic optimization problem, globally.

TABLE 1. List of the main variables.

variables	definition
$h^f_{m,n}$	Channel coefficient from BS f to the m^{th} user on subcarrier n
$h^f_{e,n}$	Channel coefficient from BS f to the e^{th} eavesdropper on subcarrier n
$p^f_{m,n}$	Transmit power of BS f to user m on subcarrier n
$\rho^f_{m,n}$	Subcarrier allocation to user m on subcarrier n in BS f
$\mathcal{F}$	Set of BSs, $\mathcal{F} = \{1, 2, ...F\}$
F	Total number of BSs
$\mathcal{N}$	Set of total subcarriers, $\mathcal{N} = \{1, 2, ...N\}$
N	Total number of subcarriers
$\mathcal{M}_f$	Set of all users in BS f, $\mathcal{M}_f = \{1, 2, ...M_f\}$
M	Total number of users, $M = \sum_{f\in\mathcal{F}} M_f$
$\mathcal{E}$	Set of all eavesdroppers, $\mathcal{E} = \{1, 2, ...E\}$
E	Total number of eavesdroppers.

D. ORGANIZATION

The remainder of this paper is organized as follows. In Section II, we present system and signal model, respectively, and explain our novel idea. Section III provides the detailed problem formulation at two scenarios: 1) Perfect CSI, 2) imperfect CSI. In Section IV, the proposed solution is expressed. The proposed scheme for ultra dense network is evaluated in Section V. Our proposed optimal solution is provided in Section VI. Multiple antennas BSs scenario is investigated in Section VII. Performance evaluation of the proposed resource allocation approach is discussed in Section VIII, before ending, the paper is concluded in Section IX.

II. SYSTEM AND SIGNAL MODEL

A. SYSTEM MODEL

In this paper, we focus on secure communication in the downlink of PD-NOMA based HetNet. As illustrated in Fig. 1, our system model consists of one MBS, and multiple SBSs. In this paper, we assume two categories of users are available: 1) Trusted users, 2) untrusted users (eavesdroppers) at which transparency of users is not clear for the BSs, i.e., they are potential eavesdroppers. In this system model, we consider two cases 1) Single antenna base station, 2) multiple antennas base stations, assume that another nodes are equipped with single antenna. For clarity, the main underutilized variables in this paper are listed in Table 1. Note that $f = 1$ refers to MBS. When BS f allocates subcarrier n to user m, the binary variable $\rho^f_{m,n} \in \{0, 1\}$ is equal to one, i.e., $\rho^f_{m,n} = 1$, and otherwise, $\rho^f_{m,n} = 0$. $h^f_{m,n} = d^{-\alpha}_{m,f}\tilde{h}^f_{m,n}$ is the channel coefficient between BS f and user m on subcarrier n, where $\tilde{h}^f_{m,n}$ indicates the Rayleigh fading, α and $d_{m,f}$ are the path loss exponent and the distance between user m and BS f, respectively. Moreover, $h^f_{e,n} = d^{-\alpha}_{e,f}\tilde{h}^f_{e,n}$. Note that the locations of BSs, legitimate users and eavesdroppers are assumed to be modeled as independent 2-D homogeneous Poisson Point Process (PPP) [35]–[37]. As mentioned, we assume two categories of users are available: 1) Trusted users, 2) untrusted users at which transparency of users is not clear for the BSs, i.e., they are potential eavesdroppers. Hence, in this paper, we assume the location of untrusted users (eavesdroppers) are perfectly known at the BSs. However, if the location of untrusted users are imperfectly known at the BSs, this scenario leads to the imperfect CSI scenario which we investigate it in Section III-B in detail.

B. SIGNAL MODEL

Employing the PD-NOMA technique, a linear combination of M_f signals is diffused by BS f to its users, [38]. In other words, BS f transmits $\sum_{j=1}^{M_f} \rho_{j,n}^f \sqrt{p_{j,n}^f} s_{j,n}^f$ on subcarrier n, where $s_{j,n}^f$ denotes the transmitted symbol of the j^{th} user on the n^{th} subcarrier by BS f. Without loss of generality, it is assumed $E\left\{\left|s_{m,n}^f\right|^2\right\} = 1, \forall m \in \mathcal{M}_f, f \in \mathcal{F}, n \in \mathcal{N}$, where $\mathcal{M}_f$, $\mathcal{N}$, and $\mathcal{F}$ are denoted set of all users in BS, set of total subcarriers, and set of BSs, respectively. Moreover, $E\{x\}$ is the expectation of x. The received signals on the m^{th} user and the e^{th} adversary, that are located in the coverage region of BS f, on the n^{th} subcarrier are expressed as

$$y_{m,n}^f = h_{m,n}^f \sum_{i \in \mathcal{M}_f} \rho_{i,n}^f \sqrt{p_{i,n}^f} s_{i,n}^f + Z_{m,n}^f + \sum_{f' \in \mathcal{F}/f} h_{m,n}^{f'} \sum_{i \in \mathcal{M}_{f'}} \rho_{i,n}^{f'} \sqrt{p_{i,n}^{f'}} s_{i,n}^{f'} \quad (1)$$

and

$$y_{e,n}^f = h_{e,n}^f \sum_{i \in \mathcal{M}_f} \rho_{i,n}^f \sqrt{p_{i,n}^f} s_{i,n}^f + Z_{e,n}^f + \sum_{f' \in \mathcal{F}/f} h_{e,n}^{f'} \sum_{i \in \mathcal{M}_{f'}} \rho_{i,n}^{f'} \sqrt{p_{i,n}^{f'}} s_{i,n}^{f'}, \quad (2)$$

respectively, where $Z_{m,n}^f \sim \mathcal{CN}\left(0, \sigma^2\right)$ and $Z_{e,n}^f \sim \mathcal{CN}\left(0, \sigma^2\right)$ are the complex Additive White Gaussian Noise (AWGN) with zero-mean and variance σ^2, on subcarrier n, over BS f, at user m and eavesdropper e, respectively.

C. ACHIEVABLE RATES AT THE LEGITIMATE USERS AND THE EAVESDROPPERS

In order to decode signals, in the PD-NOMA-based system, users apply SIC [14], [39]. In these systems, user m, firstly detects the i^{th} user's message, then removes the detected message from the received signal, in a consecutive way. When user m applies SIC, its SINR in BS f on subcarrier n can be expressed as:

$$\gamma_{m,n}^f = \frac{p_{m,n}^f \left|h_{m,n}^f\right|^2}{\left|h_{m,n}^f\right|^2 \sum_{\substack{\left|h_{m,n}^f\right|^2 \le \left|h_{i,n}^f\right|^2 \\ i \in \mathcal{M}_f/\{m\}}} p_{i,n}^f \rho_{i,n}^f + I_{m,n}^f + \sigma^2}, \quad (3)$$

where $I_{m,n}^f = \sum_{f' \in \mathcal{F}/f} \left|h_{m,n}^{f'}\right|^2 \sum_{i \in \mathcal{M}_{f'}} \rho_{i,n}^{f'} p_{i,n}^{f'}$ and its achievability rate is given by:

$$r_{m,n}^f = \log(1 + \gamma_{m,n}^f). \quad (4)$$

In the PD-NOMA-based system, users are able to perform SIC, if the following condition holds [12], [32], [33]

- SIC can be applied by user m if user i's received SINR for its signal is less than or equal to user m's received SINR for user i's signal.

In other words, user m can successfully decode and remove the i^{th} user's signal on subcarrier n in BS f, whenever the following inequality is satisfied:

$$\gamma_{m,n}^f(i) \ge \gamma_{i,n}^f(i)\, \forall i, \quad m \in \mathcal{M}_f,\ f \in \mathcal{F},\ n \in \mathcal{N}, \quad |h_{i,n}^f|^2 \le |h_{m,n}^f|^2, \quad i \ne m, \quad (5)$$

where $\gamma_{m,n}^f(i)$ is user m's SINR for user i's signal and $\gamma_{i,n}^f(i)$ is user i's SINR for its own signal. Accordingly, (5) can be rewritten as follows:

$$\begin{aligned} Q_{m,i,n}^f(\boldsymbol{\rho}, \mathbf{P}) &\triangleq -|h_{m,n}^f|^2\sigma^2 + |h_{i,n}^f|^2\sigma^2 + |h_{i,n}^f|^2 I_{m,n}^f \\ &\quad - |h_{m,n}^f|^2 I_{i,n}^f - \left|h_{m,n}^f\right|^2 \left|h_{i,n}^f\right|^2 \sum_{\substack{\left|h_{i,n}^f\right|^2 \le \left|h_{l,n}^f\right|^2 \\ l \in \mathcal{M}_f/\{i\}}} p_{l,n}^f \rho_{l,n}^f \\ &\quad + \left|h_{i,n}^f\right|^2 \left|h_{m,n}^f\right|^2 \sum_{\substack{\left|h_{m,n}^f\right|^2 \le \left|h_{l,n}^f\right|^2 \\ l \in \mathcal{M}_f/\{i\}}} p_{l,n}^f \rho_{l,n}^f \le 0. \end{aligned} \quad (6)$$

We propose a novel resource allocation algorithm in which eavesdropper is not able to employ SIC to increase its own achievable rate. In this case, eavesdropper e can not apply SIC, hence, all users' messages are treated as interference in the e^{th} eavesdropper. Therefore, SINR of the eavesdropper e in BS f on subcarrier n can be obtained as:

$$\gamma_{e,n}^{f,m} = \frac{p_{m,n}^f \left|h_{e,n}^f\right|^2}{\left|h_{e,n}^f\right|^2 \sum_{i \in \mathcal{M}_f/\{m\}} p_{i,n}^f \rho_{i,n}^f + I_{e,n}^f + \sigma^2}. \quad (7)$$

where $I_{e,n}^f = \sum_{f' \in \mathcal{F}/f} \left|h_{e,n}^{f'}\right|^2 \sum_{i \in \mathcal{M}_{f'}} \rho_{i,n}^{f'} p_{i,n}^{f'}$ and its achievable rate is given by:

$$r_{e,n}^{f,m} = \log(1 + \gamma_{e,n}^{f,m}), \quad (8)$$

For SIC avoidance at the eavesdroppers, the following inequality must be satisfied:

$$\gamma_{e,n}^{f,m}(i) \le \gamma_{i,n}^f(i), \forall i, m \in \mathcal{M}_f, e \in \mathcal{E}, f \in \mathcal{F}, n \in \mathcal{N} \quad |h_{i,n}^f|^2 \le |h_{e,n}^f|^2, \quad (9)$$

by some mathematical manipulation, (9) is equivalent to the following inequality[1]:

$$\begin{aligned}&\Psi^{f}_{m,i,n,e}(\boldsymbol{\rho},\mathbf{P})\\&\quad=-|h^{f}_{e,n}|^2\sigma^2+|h^{f}_{i,n}|^2\sigma^2-|h^{f}_{e,n}|^2 I^{f}_{i,n}\\&\qquad+|h^{f}_{i,n}|^2 I^{f}_{e,n}-\left|h^{f}_{e,n}\right|^2\left|h^{f}_{i,n}\right|^2\sum_{\substack{\left|h^{f}_{i,n}\right|^2\le\left|h^{f}_{l,n}\right|^2\\ l\in\mathcal{M}_f/\{i\}}}p^{f}_{l,n}\rho^{f}_{l,n}\\&\qquad+\left|h^{f}_{i,n}\right|^2\left|h^{f}_{e,n}\right|^2\sum_{l\in\mathcal{M}_f/\{i\}}p^{f}_{l,n}\rho^{f}_{l,n}\ge 0.\end{aligned}\tag{10}$$

In the following, we assume that the eavesdroppers are non-colluding, hence we have

$$r^{f,m}_{e_{\max},n}=\max_{e\in\mathcal{E}}\left\{\log(1+\gamma^{f,m}_{e,n})\right\},\tag{11}$$

therefore, the secrecy rare at the m^{th} user served by BS f on subcarrier n can be obtained as follows:

$$R^{\sec f}_{m,n}=\left[r^{f}_{m,n}-r^{f,m}_{e_{\max},n}\right]^{+},\tag{12}$$

where $[\Psi]^{+}=\max\{\Psi,0\}$.

III. PROBLEM FORMULATION

In this section, we propose a new policy for resource allocation to maximize the sum secrecy rate. It should be noted, in practical systems, having knowledge of all eavesdroppers' CSI is very important, hence, we investigate two cases: 1) Perfect CSI of the eavesdroppers, 2) imperfect CSI of the eavesdroppers, We investigate these two scenarios in two Subsections III-A and III-B, respectively.

A. PERFECT CSI SCENARIO

In this subsection, we assume the CSI of eavesdroppers are available at the BSs [40], [41]. Moreover, we propose a policy for resource allocation to maximize the sum secrecy rate. In this policy, unlike the users, the eavesdroppers cannot apply SIC. We formulate the considered optimization problem of sum secrecy rate maximization as (13). Since the secrecy rate cannot be negative, constraint (14) should be satisfied.

$$\max_{\mathbf{P},\boldsymbol{\rho}}\sum_{\forall f\in\mathcal{F}}\sum_{\forall m\in\mathcal{M}_f}\sum_{\forall n\in\mathcal{N}}\rho^{f}_{m,n}\left\{r^{f}_{m,n}-r^{f,m}_{e_{\max},n}\right\},\tag{13a}$$

$$\text{s.t.}:\ C_1:\ \sum_{m\in\mathcal{M}_f}\sum_{n\in\mathcal{N}}\rho^{f}_{m,n}p^{f}_{m,n}\le p^{f}_{\max}\quad\forall f\in\mathcal{F},\tag{13b}$$

$$C_2:\ \sum_{m\in\mathcal{M}_f}\rho^{f}_{m,n}\le\ell,\quad\forall n\in\mathcal{N},\ f\in\mathcal{F},\tag{13c}$$

$$C_3:\ \rho^{f}_{m,n}\in\{0,1\},\quad\forall m\in\mathcal{M}_f,\ n\in\mathcal{N},\ f\in\mathcal{F},\tag{13d}$$

$$C_4:\ p^{f}_{m,n}\ge 0,\quad\forall m\in\mathcal{M}_f,\ n\in\mathcal{N},\ f\in\mathcal{F},\tag{13e}$$

$$\begin{aligned}C_5:\ &\rho^{f}_{m,n}\rho^{f}_{i,n}Q^{f}_{m,i,n}(\boldsymbol{\rho},\ \mathbf{P})\le 0,\ \forall f\in\mathcal{F},\\&n\in\mathcal{N},\quad m,i\in\mathcal{M}_f,\ |h^{f}_{i,n}|^2\le|h^{f}_{m,n}|^2,\ i\ne m,\end{aligned}\tag{13f}$$

$$\begin{aligned}C_6:\ &\rho^{f}_{m,n}\rho^{f}_{i,n}\psi^{f}_{m,i,n,e}(\boldsymbol{\rho},\mathbf{P})\ge 0,\quad\forall f\in\mathcal{F},\ n\in\mathcal{N},\\&m,i\in\mathcal{M}_f,\quad e\in\mathcal{E},\ |h^{f}_{i,n}|^2\le|h^{f}_{e,n}|^2,\end{aligned}\tag{13g}$$

$$C_7:\ r^{f}_{m,n}-r^{f,m}_{e_{\max},n}\ge 0,\quad\forall m\in\mathcal{M}_f,\ n\in\mathcal{N},\ f\in\mathcal{F},\tag{13h}$$

The optimization variables $\mathbf{P}$ and $\boldsymbol{\rho}$ are defined as $\mathbf{P}=\left[p^{f}_{m,n}\right]$ and $\boldsymbol{\rho}=\left[\rho^{f}_{m,n}\right]\forall m\in\mathcal{M}_f,n\in\mathcal{N},f\in\mathcal{F}$, moreover $p^{f}_{\max}$ is the maximum allowable transmit power at BS f. Constraint C_1 demonstrates the maximum allowable transmit power of BS f. In order to guarantee each subcarrier can be allocated to at most ℓ users, constraint C_2 is imposed. Constraint C_4 denotes that the transmit power is non-negative. Constraint C_5 guarantees user m can perform SIC successfully on users that $|h^{f}_{i,n}|^2\le|h^{f}_{m,n}|^2$. Constraint C_6 assures that eavesdropper e is not able to perform SIC, and other users' signals are treated as interference. Constraint C_7 imposes that the secrecy rate is not never negative. It is necessary to mention that constraints C_5 and C_6 are consistent under all circumstances. In order to investigate this claim, we consider the worst circumstance in which $\gamma^{f,m}_{e,n}(i)>\gamma^{f}_{i,n}(i),\forall i,m\in\mathcal{M}_f,e\in\mathcal{E},f\in\mathcal{F},n\in\mathcal{N},|h^{f}_{i,n}|^2\le|h^{f}_{e,n}|^2$. In this considered case, the mentioned BS f does not allocate subcarrier n to user m, i.e., $\rho^{f}_{m,n}=0$, which leads to satisfying constraints C_5 and C_6.

B. IMPERFECT CSI SCENARIO

In this subsection, we assume imperfect CSI of nodes is available at the BSs.[2] In other words, the BSs have the knowledge of an estimated version of channel [42], [43], i.e., $\hat{h}^{f}_{e,n}$ and $\hat{h}^{f}_{m,n}$, and the channel estimation errors at eavesdroppers and users are defined as $e_{h^{f}_{e,n}}=\tilde{h}^{f}_{e,n}-\hat{h}^{f}_{e,n}$ and $e_{h^{f}_{m,n}}=\tilde{h}^{f}_{m,n}-\hat{h}^{f}_{m,n}$, respectively. Based on the worst case method,

[1] It is worth noting that in the multi BSs networks because of having inter-cellular interference, if eavesdropper's channel is superior to user m, the eavesdropper's received SINR for user m's signal is not necessarily more than user m's received SINR at its own signal. The reason is that if eavesdropper's channel is superior to user m, it is possible that eavesdropper receives more interference from other BSs with respect to user m, which leads to a decrease in the eavesdropper's received SINR for user m's signal.

[2] As mentioned, we assume two categories of users are available 1) Trusted users, 2) untrusted users at which transparency of users is not clear for the BSs, i.e., they are potential eavesdroppers. If the untrusted users similar to the trusted users transmit pilot signals, the BSs estimate the channels, this case leads to "perfect CSI scenario". But if the untrusted users transmit the degraded or reinforced versions of pilot signals, the BSs are not able to estimate CSI of the untrusted users perfectly which leads to "imperfect CSI scenario" i.e., the BSs can have the knowledge of an estimated version of each eavesdropping channel. Moreover, in practical systems, CSIs of legitimate users may be also imperfect due to the error of channel estimation.

the channel mismatches lie in the bounded set, i.e., $\mathbb{E}_{h_e} = \left\{e_{h^f_{e,n}} : \left|e_{h^f_{e,n}}\right|^2 \leq \epsilon_e\right\}$ $\forall e \in \mathcal{E}, n \in \mathcal{N}, f \in \mathcal{F}$, and $\mathbb{E}_{h_m} = \left\{e_{h^f_{m,n}} : \left|e_{h^f_{m,n}}\right|^2 \leq \epsilon_m\right\}$ $\forall m \in \mathcal{M}_f, n \in \mathcal{N}, f \in \mathcal{F}$, where ϵ_e and ϵ_m are known constant. Therefore, we model the channel coefficients from BS f to the e^{th} and the m^{th} user on subcarrier n as follows, respectively:

$$\left|\tilde{h}^f_{e,n}\right|^2 = \left|\hat{h}^f_{e,n} + e_{h^f_{e,n}}\right|^2, \quad \left|\tilde{h}^f_{m,n}\right|^2 = \left|\hat{h}^f_{m,n} + e_{h^f_{m,n}}\right|^2. \tag{14}$$

We focus on optimizing the worst-case performance, where we maximize the worst case sum secrecy rate for the worst channel mismatch $e_{h^f_{e,n}}$ and $e_{h^f_{m,n}}$ in the bounded set $\mathbb{E}_{h_e}$ and $\mathbb{E}_{h_m}$. Hence, the imperfect CSI optimization problem can be formulated as follows:

$$\max_{\mathbf{P},\boldsymbol{\rho}} \min_{\boldsymbol{\varepsilon_e},\boldsymbol{\varepsilon_m}} \sum_{\forall f\in\mathcal{F}} \sum_{\forall m\in\mathcal{M}_f} \sum_{\forall n\in\mathcal{N}} \rho^f_{m,n}\left\{r^f_{m,n} - r^{f,m}_{e_{\max},n}\right\}, \tag{15a}$$

$$\text{s.t.}: C_1: \sum_{m\in\mathcal{M}_f} \sum_{n\in\mathcal{N}} \rho^f_{m,n} p^f_{m,n} \leq p^f_{\max} \quad \forall f \in \mathcal{F}, \tag{15b}$$

$$C_2: \sum_{m\in\mathcal{M}_f} \rho^f_{m,n} \leq \ell, \quad \forall n \in \mathcal{N}, f \in \mathcal{F}, \tag{15c}$$

$$C_3: \rho^f_{m,n} \in \{0, 1\}, \quad \forall m \in \mathcal{M}_f, n \in \mathcal{N}, f \in \mathcal{F}, \tag{15d}$$

$$C_4: p^f_{m,n} \geq 0, \quad \forall m \in \mathcal{M}_f, n \in \mathcal{N}, f \in \mathcal{F}, \tag{15e}$$

$$C_5: \rho^f_{m,n}\rho^f_{i,n} Q^f_{m,i,n}(\boldsymbol{\rho}, \mathbf{P}) \leq 0, \quad \forall f \in \mathcal{F}, n \in \mathcal{N}, m, i \in \mathcal{M}_f, \quad |h^f_{i,n}|^2 \leq |h^f_{m,n}|^2, i \neq m, \tag{15f}$$

$$C_6: \rho^f_{m,n}\rho^f_{i,n} \psi^f_{m,i,n,e}(\boldsymbol{\rho}, \mathbf{P}) \geq 0, \quad \forall f \in \mathcal{F}, \quad n \in \mathcal{N}, m, i \in \mathcal{M}_f, \quad e \in \mathcal{E}, |h^f_{i,n}|^2 \leq |h^f_{e,n}|^2, i \neq m, \tag{15g}$$

$$C_7: r^f_{m,n} - r^{f,m}_{e_{\max},n} \geq 0, \quad \forall m \in \mathcal{M}_f, n \in \mathcal{N}, f \in \mathcal{F}, \tag{15h}$$

$$C_8: \left|e_{h^f_{e,n}}\right|^2 \leq \epsilon_e, \quad \forall f \in \mathcal{F}, n \in \mathcal{N}, e \in \mathcal{E}, \tag{15i}$$

$$C_9: \left|e_{h^f_{m,n}}\right|^2 \leq \epsilon_m, \forall f \in \mathcal{F}, \quad n \in \mathcal{N}, m \in \mathcal{M}_f, \tag{15j}$$

where the optimization variables $\boldsymbol{\varepsilon_e}$ and $\boldsymbol{\varepsilon_m}$ are defined as $\boldsymbol{\varepsilon_e} = \left[e_{h^f_{e,n}}\right], \forall e \in \mathcal{E}, n \in \mathcal{N}, f \in \mathcal{F}$ and $\boldsymbol{\varepsilon_m} = \left[e_{h^f_{m,n}}\right], \forall m \in \mathcal{M}_f, n \in \mathcal{N}, f \in \mathcal{F}$, respectively.

IV. SOLUTIONS OF THE OPTIMIZATION PROBLEM

The optimization problems (13) and (15) are non-convex because they have binary and continuous variables for subcarrier and power allocation, respectively. Besides, the objective functions are non-convex. Hence, we can not employ existing convex optimization methods straightly. Hence, to tackle this issue, we adopt the well-known alternative method [44], to solve the optimization problems.[3]

A. SOLUTION OF THE OPTIMIZATION PROBLEM IN PERFECT CSI SCENARIO

As there is the max operator in the objective function and Constraint C_7, we use a slack variable $\upsilon^f_{m,n}$ which is defined as

$$\max_{e\in\varepsilon_e} \left\{\log(1 + \gamma^{f,m}_{e,n})\right\} = \upsilon^f_{m,n}, \tag{16}$$

by applying the epigraph method, the optimization problem (13) is rewritten as

$$\max_{\mathbf{P},\boldsymbol{\rho},\boldsymbol{\upsilon}} \sum_{\forall f\in\mathcal{F}} \sum_{\forall m\in\mathcal{M}_f} \sum_{\forall n\in\mathcal{N}} \rho^f_{m,n}\left\{r^f_{m,n} - \upsilon^f_{m,n}\right\}, \tag{17a}$$

$$\text{s.t.}: C_1 - C_6, \quad C'_7: \left\{r^f_{m,n} - \upsilon^f_{m,n}\right\} \geq 0, \quad \forall m \in \mathcal{M}_f, n \in \mathcal{N}, f \in \mathcal{F}, \tag{17b}$$

$$C'_8: \log\left(1 + \gamma^{f,m}_{e,n}\right) \leq \upsilon^f_{m,n} \quad \forall e \in \mathcal{E}, n \in \mathcal{N}, f \in \mathcal{F}, \quad \forall m \in \mathcal{M}_f, \tag{17c}$$

where $\boldsymbol{\upsilon}$ is defined as $\boldsymbol{\upsilon} = \left[\upsilon^f_{m,n}\right], \forall m \in \mathcal{M}_f, n \in \mathcal{N}, f \in \mathcal{F}$. For solving (17), we adopt the well-known iterative algorithm called ASM. In this method, the optimization problems are converted to two subproblems which one of them has binary and another has continuous optimization variables, in other words, power and subcarrier are allocated alternatively [45]. In this method, in each iteration, we allocate transmit power and subcarriers, separately. In other words, in this iterative method, in each iteration we consider fixed subcarrier and allocate power, then, for subcarrier allocation we consider fixed power. We summarize the explained algorithm in Algorithm 1. As seen in this algorithm, it is ended when the stopping condition is satisfied i.e., $\|\mathbf{P}(\mu + 1) - \mathbf{P}(\mu)\| \leq \Theta$, where μ and Θ are the iteration number and stopping threshold, respectively.

1) INITIALIZATION METHOD

In order to begin the algorithm, we need to initial vectors $\mathbf{P}$ and $\boldsymbol{\rho}$. For initialization, it is supposed that the SBSs do not transmit data, i.e., SBSs at initialization do not serve any users [46], [47]. In other words, $p^f_{m,n} = 0 \ \forall f \in \mathcal{F}/\{0\}$. Moreover, the subcarriers are allocated to one MBS user that has the highest secrecy rate.

[3]Please note that our aim is to design a strategy to prevent eavesdroppers from using SIC. Hence, we employ the well-known method and approximation to solve our proposed optimization problem. It is worth noting that we compare the output of employed methods with the optimal solution which is obtained by the high complex polyblock algorithm, however, the employed method is low complex and its optimality gap is small.

Algorithm 1 Iterative Resource Allocation Algorithm for Perfect CSI

1: Reformulate the optimization problem via the epigraph method
2: Initialization: Set $\mu = 0$ (μ is the iteration number) and initialize to $\boldsymbol{\rho}(0)$ and $\mathbf{P}(0)$.
3: Set $\boldsymbol{\rho} = \boldsymbol{\rho}(\mu)$,
4: Solve (43) and set the result to $\mathbf{P}(\mu+1)$,
5: Solve (18) and set the result to $\boldsymbol{\rho}(\mu+1)$,
6: If $\|\mathbf{P}(\mu+1) - \mathbf{P}(\mu)\| \leq \Theta$
stop,
else
set $\mu = \mu + 1$ and go back to step 3.

2) SUBCARRIER ALLOCATION

The subproblem for subcarrier allocation with fixed transmit power (which are computed in the previous iteration) is expressed as:

$$\max_{\boldsymbol{\rho}} \sum_{\forall f \in \mathcal{F}} \sum_{\forall m \in \mathcal{M}_f} \sum_{\forall n \in \mathcal{N}} \rho^f_{m,n} \left\{ r^f_{m,n} - \upsilon^f_{m,n} \right\},$$
$$\text{s.t.:} \quad C_1 - C_3, C_5, C_6, C_7', C_8'. \tag{18}$$

Since this optimization problem is Integer Nonlinear Programming (INLP), we can solve it by exploiting MADS, to this end, we employ the NOMAD solver [48].

3) POWER ALLOCATION

The power allocation subproblem at each iteration when the subcarriers allocation variables are fixed, is expressed as

$$\max_{\mathbf{P},\boldsymbol{\upsilon}} \sum_{\forall f \in \mathcal{F}} \sum_{\forall m \in \mathcal{M}_f} \sum_{\forall n \in \mathcal{N}} \rho^f_{m,n} \left\{ r^f_{m,n} - \upsilon^f_{m,n} \right\},$$
$$\text{s.t.:} \quad C_1, C_4 - C_6, C_7', C_8'. \tag{19}$$

This optimization subproblem is non-convex because constraint C_8' is non-convex, the objective function and constraint C_7' are non-concave. To tackle this difficulty, we utilize the SCA approach to approximate constraints C_8' and the objective function.

First, we investigate C_8':

$$C_8' : \log\left(1 + \gamma^{f,m}_{e,n}\right) \leq \upsilon^f_{m,n}, \tag{20}$$

by substitution (7) into (20), we have

$$\log\left(1 + \frac{p^f_{m,n}\left|h^f_{e,n}\right|^2}{\left|h^f_{e,n}\right|^2 \sum\limits_{i \in \mathcal{M}_f/\{m\}} p^f_{i,n}\rho^f_{i,n} + I^f_{e,n} + \sigma^2}\right) - \upsilon^f_{m,n} \leq 0, \tag{21}$$

the left hand side of (21) is written as follows:

$$\log\left(\left|h^f_{e,n}\right|^2 \sum_{i \in \mathcal{M}_f/\{m\}} p^f_{i,n}\rho^f_{i,n} + I^f_{e,n} + \sigma^2 + p^f_{m,n}\left|h^f_{e,n}\right|^2\right)$$
$$- \log\left(\left|h^f_{e,n}\right|^2 \sum_{i \in \mathcal{M}_f/\{m\}} p^f_{i,n}\rho^f_{i,n} + I^f_{e,n} + \sigma^2\right) - \upsilon^f_{m,n}. \tag{22}$$

As seen, (22) is the difference between two concave functions. Hence, we can employ the DC method to approximate (22) to a convex constraint. To this end, we write (22) as follows:

$$\Xi^{f,m}_{e,n}(\mathbf{P}) = \Im^{f,m}_{e,n}(\mathbf{P}) - \Phi^{f,m}_{e,n}(\mathbf{P}), \tag{23}$$

where

$$\Im^{f,m}_{e,n}(\mathbf{P}) = -\log\left(\left|h^f_{e,n}\right|^2 \sum_{i \in \mathcal{M}_f/\{m\}} p^f_{i,n}\rho^f_{i,n} + I^f_{e,n} + \sigma^2\right) - \upsilon^f_{m,n}, \tag{24}$$

and

$$\Phi^{f,m}_{e,n}(\mathbf{P}) = -\log\left(\left|h^f_{e,n}\right|^2 \sum_{i \in \mathcal{M}_f/\{m\}} p^f_{i,n}\rho^f_{i,n} + p^f_{m,n}\left|h^f_{e,n}\right|^2 + I^f_{e,n} + \sigma^2\right) \tag{25}$$

$\Im^{f,m}_{e,n}(\mathbf{P})$ and $\Phi^{f,m}_{e,n}(\mathbf{P})$ are convex, by utilizing a linear approximation, $\Phi^{f,m}_{e,n}(\mathbf{P})$ can be written as follows:

$$\Phi^{f,m}_{e,n}(\mathbf{P}) \simeq \tilde{\Phi}^{f,m}_{e,n}(\mathbf{P}) = \Phi^{f,m}_{e,n}(\mathbf{P}(\mu-1)) + \nabla^T \Phi^{f,m}_{e,n}(\mathbf{P}(\mu-1))(\mathbf{P} - \mathbf{P}(\mu-1)),$$

where $\nabla\Phi^{f,m}_{e,n}(\mathbf{P})$, is the gradient of $\Phi^{f,m}_{e,n}(\mathbf{P})$ which is defined as:

$$\nabla\Phi^{f,m}_{e,n}(\mathbf{P}) = \frac{\partial}{\partial \mathbf{P}} \Phi^{f,m}_{e,n}(\mathbf{P}) = \left[\frac{\partial \Phi^{f,m}_{e,n}(\mathbf{P})}{\partial p^f_{m,n}}\right], \quad \forall m \in \mathcal{M}_f, \ \forall n \in \mathcal{N}, \ \forall f \in \mathcal{F}, \ \forall e \in \mathcal{E}, \tag{26}$$

and

$$\frac{\partial \Phi^{f,m}_{e,n}(\mathbf{P})}{\partial p^c_{a,b}} = \begin{cases} X, & a = m, b = n, c = f, \\ Y, & \forall a \in \mathcal{M}_f/\{m\}, b = n, c = f, \\ B, & \forall a \in \mathcal{M}_{f'}, b = n, c = f' \in \mathcal{F}/f, \\ 0, & O.W, \end{cases} \tag{27}$$

moreover, X, Y, and B are calculated as follows:

$$X = -\frac{\left|h^f_{e,n}\right|^2}{\left|h^f_{e,n}\right|^2 \sum\limits_{i \in \mathcal{M}_f/\{m\}} p^f_{i,n}\rho^f_{i,n} + p^f_{m,n}\left|h^f_{e,n}\right|^2 + I^f_{e,n} + \sigma^2}, \tag{28}$$

$$Y = -\frac{\left|h^f_{e,n}\right|^2 \rho^f_{a,n}}{\left|h^f_{e,n}\right|^2 \sum_{i\in\mathcal{M}_f/\{m\}} p^f_{i,n}\rho^f_{i,n} + p^f_{m,n}\left|h^f_{e,n}\right|^2 + I^f_{e,n} + \sigma^2}, \tag{29}$$

$$B = -\frac{\left|h^c_{e,n}\right|^2 \rho^c_{a,n}}{\left|h^f_{e,n}\right|^2 \sum_{i\in\mathcal{M}_f/\{m\}} p^f_{i,n}\rho^f_{i,n} + p^f_{m,n}\left|h^f_{e,n}\right|^2 + I^f_{e,n} + \sigma^2}, \tag{30}$$

therefore, $\nabla^T \Phi^{f,m}_{e,n}(\mathbf{P})$ is a vector that its length is $N \times M \times F$. After approximation C'_8 to the convex constraint, we convert the objective function and constraint C'_7 to a concave function and concave constrain, respectively, by exploiting the DC method, hence we have:

$$\log(1+\gamma^f_{m,n}) - \upsilon^f_{m,n}, \tag{31}$$

by substitution (3) into (31), we have

$$\log(1+\frac{p^f_{m,n}\left|h^f_{m,n}\right|^2}{\left|h^f_{m,n}\right|^2 \sum_{\substack{\left|h^f_{m,n}\right|^2 \le \left|h^f_{i,n}\right|^2 \\ i\in\mathcal{M}_f/\{m\}}} p^f_{i,n}\rho^f_{i,n} + I^f_{m,n} + \sigma^2}) - \upsilon^f_{m,n}, \tag{32}$$

where can be written as:

$$\log(\left|h^f_{m,n}\right|^2 \sum_{\substack{\left|h^f_{m,n}\right|^2 \le \left|h^f_{i,n}\right|^2 \\ i\in\mathcal{M}_f/\{m\}}} p^f_{i,n}\rho^f_{i,n} + I^f_{m,n} + \sigma^2 + p^f_{m,n}\left|h^f_{m,n}\right|^2) - \log(\left|h^f_{m,n}\right|^2 \sum_{\substack{\left|h^f_{m,n}\right|^2 \le \left|h^f_{i,n}\right|^2 \\ i\in\mathcal{M}_f/\{m\}}} p^f_{i,n}\rho^f_{i,n} + I^f_{m,n} + \sigma^2) - \upsilon^f_{m,n}, \tag{33}$$

we can writhe (33) as follows:

$$U^f_{m,n}(\mathbf{P}) = G^f_{m,n}(\mathbf{P}) - H^f_{m,n}(\mathbf{P}), \tag{34}$$

where $H^f_{m,n}(\mathbf{P})$ and $G^f_{m,n}(\mathbf{P})$ are defined as

$$G^f_{m,n}(\mathbf{P}) = -\upsilon^f_{m,n} + \log \tag{35}$$

$$\times(\left|h^f_{m,n}\right|^2 \sum_{\substack{\left|h^f_{m,n}\right|^2 \le \left|h^f_{i,n}\right|^2 \\ i\in\mathcal{M}_f/\{m\}}} p^f_{i,n}\rho^f_{i,n} + p^f_{m,n}\left|h^f_{m,n}\right|^2 + I^f_{m,n} + \sigma^2), \tag{36}$$

and

$$H^f_{m,n}(\mathbf{P}) = \log\left(\left|h^f_{m,n}\right|^2 \sum_{\substack{\left|h^f_{m,n}\right|^2 \le \left|h^f_{i,n}\right|^2 \\ i\in\mathcal{M}_f/\{m\}}} p^f_{i,n}\rho^f_{i,n} + I^f_{m,n} + \sigma^2\right), \tag{37}$$

respectively. $G^f_{m,n}(\mathbf{P})$ and $H^f_{m,n}(\mathbf{P})$ are concave, by utilizing a linear approximation we can write $H^f_{m,n}(\mathbf{P})$ as follows:

$$H^f_{m,n}(\mathbf{P}) \simeq \tilde{H}^f_{m,n}(\mathbf{P}) = H^f_{m,n}(\mathbf{P}(\mu-1)) + \nabla^T H^f_{m,n}(\mathbf{P}(\mu-1))(\mathbf{P} - \mathbf{P}(\mu-1)), \tag{38}$$

where $\nabla^T H^f_{m,n}(\mathbf{P})$ is calculated as follows:

$$\nabla^T H^f_{m,n}(\mathbf{P}) = \frac{\partial}{\partial \mathbf{P}} H^f_{m,n}(\mathbf{P}) = \left[\frac{\partial H^f_{m,n}(\mathbf{P})}{\partial p^f_{m,n}}\right], \quad \forall m \in \mathcal{M}_f,\ \forall n \in \mathcal{N},\ \forall f \in \mathcal{F}, \tag{39}$$

We take derivative of $H^f_{m,n}(\mathbf{P})$ with respect to $p^c_{a,b}$ as follows:

$$\frac{\partial H^f_{m,n}(\mathbf{P})}{\partial p^c_{a,b}} = \begin{cases} Z & \forall a \in \mathcal{M}_f/\{m\}, b=n, c=f, \left|h^f_{m,n}\right|^2 \le \left|h^f_{a,n}\right|^2, \\ T & \forall a \in \mathcal{M}_{f'}, b=n, c=f' \in \mathcal{F}/f \\ 0 & O.W \end{cases} \tag{40}$$

where Z and T are calculated as follows:

$$Z = \frac{\left|h^f_{m,n}\right|^2 \rho^f_{a,n}}{\left|h^f_{m,n}\right|^2 \sum_{\substack{\left|h^f_{m,n}\right|^2 \le \left|h^f_{i,n}\right|^2 \\ i\in\mathcal{M}_f/\{m\}}} p^f_{i,n}\rho^f_{i,n} + I^f_{m,n} + \sigma^2}, \tag{41}$$

$$T = \frac{\left|h^c_{m,n}\right|^2 \rho^c_{a,n}}{\left|h^f_{m,n}\right|^2 \sum_{\substack{\left|h^f_{m,n}\right|^2 \le \left|h^f_{i,n}\right|^2 \\ i\in\mathcal{M}_f/\{m\}}} p^f_{i,n}\rho^f_{i,n} + I^f_{m,n} + \sigma^2}. \tag{42}$$

Consequently, we have a convex optimization problem in the canonical form, by exploiting the DC approximation, which is formulated as:

$$\max_{\mathbf{P},\boldsymbol{\upsilon}} \sum_{\forall f\in\mathcal{F}} \sum_{\forall m\in\mathcal{M}_f} \sum_{\forall n\in\mathcal{N}} \rho^f_{m,n}\left\{G^f_{m,n}(\mathbf{P}) - \tilde{H}^f_{m,n}(\mathbf{P})\right\}, \tag{43a}$$

$$\text{s.t.:}\quad C_1 - C_6, \tag{43b}$$

$$C'_7:\quad G^f_{m,n}(\mathbf{P}) - \tilde{H}^f_{m,n}(\mathbf{P}) \ge 0, \quad \forall m \in \mathcal{M}_f, \; n \in \mathcal{N}, f \in \mathcal{F}, \tag{43c}$$

$$C'_8:\quad \Im^{f,m}_{e,n}(\mathbf{P}) - \tilde{\Phi}^{f,m}_{e,n}(\mathbf{P}) \le 0 \quad \forall e \in \mathcal{E}, \; n \in \mathcal{N}, f \in \mathcal{F}, m \in \mathcal{M}_f, \tag{43d}$$

For solving the convex optimization problem (43), we can use available softwares, such as CVX solver [49].

4) CONVERGENCE OF THE ALGORITHM

In this subsection, we prove the convergence of the algorithm and illustrate that after each iteration the value of objective function $f(\boldsymbol{\rho}, \mathbf{P}) = \rho^f_{m,n}\left\{r^f_{m,n} - \upsilon^{f,m}_{e,n}\right\}$, is improved and converged.

Proof: In this algorithm, after applying the third step, with a given $\boldsymbol{\rho} = \boldsymbol{\rho}(\mu)$, the power allocation of iteration $\mu + 1$ is obtained. According to Appendix I, we will have $f(\boldsymbol{\rho}(\mu), \mathbf{P}(\mu)) \leq f(\boldsymbol{\rho}(\mu), \mathbf{P}(\mu+1))$. Moreover, in the fourth step, with a given $\mathbf{P} = \mathbf{P}(\mu+1)$, the subcarrier allocation of this iteration is obtained. According to this fact that, after each iteration, subcarrier allocation with feasible power solution improves the objective function, hence we have:

$$\begin{aligned} \ldots \leq f(\boldsymbol{\rho}(\mu), \mathbf{P}(\mu)) &\leq f(\boldsymbol{\rho}(\mu), \mathbf{P}(\mu+1)) \\ &\leq f(\boldsymbol{\rho}(\mu+1), \mathbf{P}(\mu+1)) \\ &\leq \ldots \leq f\left(\boldsymbol{\rho}^*, \mathbf{P}^*\right) \end{aligned} \tag{44}$$

where $\boldsymbol{\rho}^*$ and $\mathbf{P}^*$ are obtained at the last iteration, [50]. Convergence behavior of the proposed algorithm is shown in Fig. 6. It should be noted, globally optimal solution is not guaranteed by this solution even after convergence. Hence, for finding the globally optimal solution, we utilize the monotonic optimization method which is explained, in Section VI.

5) COMPUTATIONAL COMPLEXITY

Solution of the optimization problem (13) consists of two stages 1) Calculation of power allocation from problem (43), 2) calculation of subcarrier allocation from problem (18). As we know, CVX software employs geometric programing with the Interior Point Method (IPM) [49], hence, the order of computational complexity can be obtained as:

$$O\left(\frac{\log\left(\frac{NOC}{t\partial}\right)}{\log(\xi)}\right), \tag{45}$$

where NOC is the total number of constraints. ∂, ξ and t are parameters of IPM. $0 \leq \partial << 1$ is the stopping criterion of IPM, ξ is used for the accuracy IPM and t is initial point for approximated the accuracy of IPM, [46], [51]. Hence, the complexity order is given by:

$$O\left(\frac{\log\left(\frac{F(1+N(1+M+M(M-1)+ME(M-1)+ME))}{t\partial}\right)}{\log(\xi)}\right) \tag{46}$$

B. SOLUTION OF THE OPTIMIZATION PROBLEM IN IMPERFECT CSI SCENARIO

For solving (15), first we solve the inner minimization and obtain $\boldsymbol{\varepsilon_e}$ and $\boldsymbol{\varepsilon_m}$, then solve the maximization problem according to Section IV-A. The inner minimization can be written as follows:

$$\min_{\boldsymbol{\varepsilon_e},\boldsymbol{\varepsilon_m}} \sum_{\forall f\in\mathcal{F}} \sum_{\forall m\in\mathcal{M}_f} \sum_{\forall n\in\mathcal{N}} \rho^f_{m,n}\left\{r^f_{m,n} - \upsilon^f_{m,n}\right\}, \tag{47a}$$

$$\text{s.t.:} \quad C_5, C_6, C_8, C_9, C'_7, C'_8. \tag{47b}$$

Our aim is to minimize the objective function, to this end, we should maximize $\upsilon^f_{m,n}$ and minimize $r^f_{m,n}$. Hence, in order to maximize $\upsilon^f_{m,n}$, according to C'_8, we maximize lower bound of $\upsilon^f_{m,n}$, i.e., $\log\left(1+\gamma^{f,m}_{e,n}\right)$. Since the logarithmic function is increasing, we can maximize $\gamma^{f,m}_{e,n}$ instead of $\log\left(1+\gamma^{f,m}_{e,n}\right)$. As $\gamma^{f,m}_{e,n}$ is fractional, we should maximize the numerator and minimize the denominator. To this end, we use the triangle inequality which is defined as follows:

$$\begin{aligned} \left|\hat{h}^f_{e,n}\right|^2 - \epsilon_e \leq \left|\hat{h}^f_{e,n}\right|^2 - \left|e_{h^f_{e,n}}\right|^2 &\leq \left|\hat{h}^f_{e,n} + e_{h^f_{e,n}}\right|^2 \\ \leq \left|\hat{h}^f_{e,n}\right|^2 + \left|e_{h^f_{e,n}}\right|^2 &\leq \left|\hat{h}^f_{e,n}\right|^2 + \epsilon_e. \end{aligned} \tag{48}$$

By using (48), we can write the upper bound of $\gamma^{f,m}_{e,n}$ as follows:

$$\begin{aligned} \gamma^f_{e,n} &= \frac{p^f_{m,n}\left|h^f_{e,n}\right|^2}{\left|h^f_{e,n}\right|^2 \sum\limits_{i\in\mathcal{M}_f/\{m\}} p^f_{i,n}\rho^f_{i,n} + I^f_{e,n} + \sigma^2} \leq \tilde{\gamma}^f_{e,n} \\ &= \frac{p^f_{m,n}\left(\left|\hat{h}^f_{e,n}\right|^2 + \epsilon_e\right)}{\left(\left|\hat{h}^f_{e,n}\right|^2 - \epsilon_e\right) \sum\limits_{i\in\mathcal{M}_f/\{m\}} p^f_{i,n}\rho^f_{i,n} + \tilde{I}^f_{e,n} + \sigma^2}. \end{aligned} \tag{49}$$

where $\tilde{I}^f_{e,n} = \sum\limits_{f'\in\mathcal{F}/f}\left(\left|\hat{h}^{f'}_{e,n}\right|^2 - \epsilon_e\right)\sum\limits_{i\in\mathcal{M}_{f'}} \rho^{f'}_{i,n}p^{f'}_{i,n}$. Also, we consider the worst case for constraint C_6. According to (48), we can rewrite the worst case C_6 as follows:

$$\begin{aligned} &\Psi^f_{m,i,n,e}(\boldsymbol{\rho}, \mathbf{P}) \\ &\geq \tilde{\Psi}^f_{m,i,n,e}(\boldsymbol{\rho}, \mathbf{P}) = \left(\left|\hat{h}^f_{i,n}\right|^2 - \epsilon_m\right)\sigma^2 \\ &+ \left(\left|\hat{h}^f_{i,n}\right|^2 - \epsilon_m\right)\tilde{I}^f_{e,n} - \left(\left|\hat{h}^f_{e,n}\right|^2 + \epsilon_e\right) \\ &\times \left(\left(\left|\hat{h}^f_{i,n}\right|^2 + \epsilon_m\right) \sum_{\substack{\left|\hat{h}^f_{i,n}\right|^2 - \epsilon_m \leq \left|\hat{h}^f_{l,n}\right|^2 + \epsilon_m \\ l\in\mathcal{M}_f/\{i\}}} p^f_{l,n}\rho^f_{l,n} + \tilde{I}^f_{i,n} + \sigma^2\right) \\ &+ \left(\left|\hat{h}^f_{e,n}\right|^2 - \epsilon_e\right)\left(\left|\hat{h}^f_{i,n}\right|^2 - \epsilon_m\right) \sum_{l\in\mathcal{M}_f/\{i\}} p^f_{l,n}\rho^f_{l,n} \geq 0. \end{aligned} \tag{50}$$

Moreover, in order to minimize $r^f_{m,n}$, we minimize $\gamma^f_{m,n}$. As $\gamma^{f,m}_{m,n}$ is fractional, we should minimize the numerator and maximize the denominator. To this end, we employ the triangle inequality as follows:

$$\gamma^f_{m,n} = \frac{p^f_{m,n}\left|h^f_{m,n}\right|^2}{\left|h^f_{m,n}\right|^2 \sum\limits_{\substack{\left|h^f_{m,n}\right|^2 \leq \left|h^f_{i,n}\right|^2 \\ i\in\mathcal{M}_f/\{m\}}} p^f_{i,n}\rho^f_{i,n} + I^f_{m,n} + \sigma^2} \geq \tilde{\gamma}^f_{m,n}$$

$$= \frac{p^f_{m,n}(\left|\hat{h}^f_{m,n}\right|^2 - \epsilon_m)}{(\left|\hat{h}^f_{m,n}\right|^2 + \epsilon_m) \sum\limits_{\substack{\left|\hat{h}^f_{m,n}\right|^2 - \epsilon_m \leq \left|\hat{h}^f_{i,n}\right|^2 + \epsilon_m \\ i \in \mathcal{M}_f/\{m\}}} p^f_{i,n}\rho^f_{i,n} + \tilde{I}^f_{m,n} + \sigma^2}, \tag{51}$$

where $\tilde{I}^f_{m,n} = \sum\limits_{f' \in F/f} \left(\left|\hat{h}^f_{m,n}\right|^2 + \epsilon_m\right) \sum\limits_{i \in M_{f'}} \rho^{f'}_{i,n} p^{f'}_{i,n}$. Also, we consider the worst case for constraint C_5. Therefore, we can rewrite the worst case C_5 as follows:

$$\begin{aligned} & Q^f_{m,i,n}(\boldsymbol{\rho}, \mathbf{P}) \\ & \leq \tilde{Q}^f_{m,i,n}(\boldsymbol{\rho}, \mathbf{P}) = -\left(\left|\hat{h}^f_{m,n}\right|^2 - \epsilon_m\right)\sigma^2 \\ & \quad + \left(\left|\hat{h}^f_{i,n}\right|^2 + \epsilon_m\right)\sigma^2 + \left(\left|\hat{h}^f_{i,n}\right|^2 + \epsilon_m\right)\tilde{I}^f_{m,n} \\ & \quad - \left(\left|\hat{h}^f_{m,n}\right|^2 - \epsilon_m\right)\tilde{I}^f_{i,n} - \left(\left|\hat{h}^f_{i,n}\right|^2 - \epsilon_m\right) \\ & \quad \times \left(\left|\hat{h}^f_{m,n}\right|^2 - \epsilon_m\right) \sum_{\substack{\left|\hat{h}^f_{i,n}\right|^2 + \epsilon_m \leq \left|\hat{h}^f_{l,n}\right|^2 - \epsilon_m \\ l \in \mathcal{M}_f/\{i\}}} p^f_{l,n}\rho^f_{l,n} + \left(\left|\hat{h}^f_{m,n}\right|^2 + \epsilon_m\right) \\ & \quad \times \left(\left|\hat{h}^f_{i,n}\right|^2 + \epsilon_m\right) \sum_{\substack{\left|\hat{h}^f_{m,n}\right|^2 - \epsilon_m \leq \left|\hat{h}^f_{l,n}\right|^2 + \epsilon_m \\ l \in \mathcal{M}_f/\{i\}}} p^f_{l,n}\rho^f_{l,n} \leq 0. \end{aligned} \tag{52}$$

In the following, we should solve the outer maximization, which is written as follows:

$$\max_{\mathbf{P},\boldsymbol{\rho},\boldsymbol{\upsilon}} \sum_{\forall f \in \mathcal{F}} \sum_{\forall m \in \mathcal{M}_f} \sum_{\forall n \in \mathcal{N}} \rho^f_{m,n} \left\{\tilde{r}^f_{m,n} - \upsilon^f_{m,n}\right\}, \tag{53a}$$

$$\text{s.t.:} \quad C_1 - C_4 \tag{53b}$$

$$C'_5: \quad \rho^f_{m,n}\rho^f_{i,n}\tilde{Q}^f_{m,i,n}(\boldsymbol{\rho}, \mathbf{P}) \leq 0, \ \forall f \in \mathcal{F}, \quad n \in \mathcal{N}, m, i \in \mathcal{M}_f, \quad |h^f_{i,n}|^2 \leq |h^f_{m,n}|^2, \ i \neq m, \tag{53c}$$

$$C'_6: \quad \rho^f_{m,n}\rho^f_{i,n}\tilde{\psi}^f_{m,i,n,e}(\boldsymbol{\rho}, \mathbf{P}) \geq 0, \quad \forall f \in \mathcal{F}, n \in \mathcal{N}, \quad m, i \in \mathcal{M}_f, \quad e \in \mathcal{E}, \ |h^f_{i,n}|^2 \leq |h^f_{e,n}|^2, \ i \neq m, \tag{53d}$$

$$C''_7: \quad \left\{\tilde{r}^f_{m,n} - \upsilon^f_{m,n}\right\} \geq 0, \quad \forall m \in \mathcal{M}_f, n \in \mathcal{N}, f \in \mathcal{F}, \tag{53e}$$

$$C''_8: \quad \log\left(1 + \tilde{\gamma}^{f,m}_{e,n}\right) \leq \upsilon^f_{m,n} \quad \forall e \in \mathcal{E}, n \in \mathcal{N}, \quad f \in \mathcal{F}, \quad \forall m \in \mathcal{M}_f, \tag{53f}$$

The optimization problem (53) can be solved similar to the proposed approach in Section IV-A.

V. MASSIVE CONNECTIVITY SCENARIO

In this section, we aim to evaluate the PD-NOMA technique in ultra dense network for secure massive connectivity in 5G networks. Without loss of generality, for changing our scenario from HetNet to HUDN, we need to extend the dimension of system model. According to [3], [29], and [52], in order to tackle high dimension complexity of resource allocation in HUDNs and overcome hardware computation limitations, it is assumed that the transmit power is uniformly allocated to devices/users and subcarriers are dynamically allocated.

To know the performance degradation due to the uniform power allocation, we compare the uniform power allocation method for a small network dimension with our proposed solution i.e., joint power and subcarrier allocation in section of simulation result. Based on simulation results, we show the performance of uniform power allocation is close to the performance of our proposed solution i.e., joint power and subcarrier allocation in the small network dimension.

VI. OPTIMAL SOLUTION

In this section, our aim is to find optimal solution for the optimization problem (17) by utilizing the monotonic optimization method.

Note that, a monotonic optimization problem in the canonical form is formulated as:

$$\begin{aligned} & \max_{x} \ g(x) \\ & s.t. \ x \in \Upsilon_1 \cap \Upsilon_2, \end{aligned} \tag{54}$$

where $g(x)$ is an increasing function, Υ_1 is a normal set with non-empty interior, and Υ_2 is a co-normal set. Hence, the optimization problem (17) is not in this form, because of existence of binary variables and non increasing objective function. Hence, three main steps should be performed as follows:

1) Problem (17) is transformed into an optimization problem at which its optimization variables are only transmit power.
2) The new optimization problem is converted to a canonical form of monotonic optimization problem.
3) Finally, by exploiting the polyblock algorithm, we solve the monotonic optimization problem globally.

A. PROBLEM TRANSFORMATION

For the first step, we transform (17) into an optimization problem at which its optimization variables are only transmit power. Based on constraints (13c) and (14), if $\underbrace{p^f_{m,n} = 0, \ldots, \text{and } p^f_{i,n} = 0}_{\ell}$, we have $p^f_{w,n} = 0$, $\forall m, \ldots, i, w \in \mathcal{M}_f$, $m \neq i \neq w$. Therefore, constraint (13c) is equivalent to the following constraint

$$\underbrace{p^f_{m,n} \times \ldots \times p^f_{i,n} \times p^f_{w,n}}_{\ell+1} \leq 0, \quad \forall n \in \mathcal{N}, f \in \mathcal{F} \quad m, \ldots, i, \quad w \in \mathcal{M}_f, \ m \neq \ldots \neq i \neq w. \tag{55}$$

Therefore, the optimization problem (17) can be transformed into a new optimization problem with only transmit power variables as follows:

$$\max_{\mathbf{P},\boldsymbol{\upsilon}} \sum_{\forall f\in\mathcal{F}}\sum_{\forall m\in\mathcal{M}_f}\sum_{\forall n\in\mathcal{N}}\left\{\tilde{r}^f_{m,n}-\upsilon^f_{m,n}\right\}, \tag{56a}$$

$$\text{s.t.:} \sum_{m\in\mathcal{M}_f}\sum_{n\in\mathcal{N}} p^f_{m,n}\le p^f_{\max} \quad \forall f\in\mathcal{F}, \tag{56b}$$

$$p^f_{m,n}\ge 0, \quad \forall m\in\mathcal{M}_f,\ n\in\mathcal{N},\ m\in\mathcal{M}_f, \tag{56c}$$

$$p^f_{m,n}p^f_{i,n}\hat{\mathcal{Q}}^f_{m,i,n}\le 0, \quad \forall f\in\mathcal{F}, \tag{56d}$$
$$n\in\mathcal{N},\ m,i\in\mathcal{M}_f,\quad |h^f_{i,n}|^2\le|h^f_{m,n}|^2,\ i\neq m,$$

$$-p^f_{m,n}p^f_{i,n}\hat{\psi}^f_{m,i,n,e}\le 0,\quad \forall f\in\mathcal{F},\ n\in\mathcal{N}, \tag{56e}$$
$$m,i\in\mathcal{M}_f,\quad e\in\mathcal{E},\ |h^f_{i,n}|^2\le|h^f_{e,n}|^2,$$

$$\log\Big(\left|h^f_{e,n}\right|^2\sum_{i\in\mathcal{M}_f/\{m\}}p^f_{i,n}+\hat{I}^f_{m,n}+\sigma^2+p^f_{m,n}\left|h^f_{e,n}\right|^2\Big)$$
$$-\log\Big(\left|h^f_{e,n}\right|^2\sum_{i\in\mathcal{M}_f/\{m\}}p^f_{i,n}+\hat{I}^f_{m,n}+\sigma^2\Big)$$
$$-\upsilon^f_{m,n}\le 0,\quad \forall e\in\mathcal{E},\ n\in\mathcal{N},\ f\in\mathcal{F},\quad \forall m\in\mathcal{M}_f, \tag{56f}$$

$$\underbrace{p^f_{m,n}\times\ldots\times p^f_{i,n}\times p^f_{w,n}}_{\ell+1}\le 0,\quad \forall n\in\mathcal{N},\ f\in\mathcal{F} \tag{56g}$$
$$m,\ldots,i,\quad w\in\mathcal{M}_f,\ m\neq\ldots\neq i\neq w.$$

where

$$\hat{\mathcal{Q}}^f_{m,i,n}=-|h^f_{m,n}|^2\sigma^2+|h^f_{i,n}|^2\sigma^2+|h^f_{i,n}|^2\hat{I}^f_{m,n} -|h^f_{m,n}|^2\hat{I}^f_{i,n}-\left|h^f_{m,n}\right|^2\left|h^f_{i,n}\right|^2\sum_{\substack{|h^f_{i,n}|^2\le|h^f_{l,n}|^2\\ l\in\mathcal{M}_f/\{i\}}}p^f_{l,n} +\left|h^f_{i,n}\right|^2\left|h^f_{m,n}\right|^2\sum_{\substack{|h^f_{m,n}|^2\le|h^f_{l,n}|^2\\ l\in\mathcal{M}_f/\{i\}}}p^f_{l,n}, \tag{57}$$

and

$$\hat{\psi}^f_{m,i,n,e}=-|h^f_{e,n}|^2\sigma^2+|h^f_{i,n}|^2\sigma^2-|h^f_{e,n}|^2\hat{I}^f_{i,n}+|h^f_{i,n}|^2\hat{I}^f_{e,n} -\left|h^f_{e,n}\right|^2\left|h^f_{i,n}\right|^2\sum_{\substack{|h^f_{i,n}|^2\le|h^f_{l,n}|^2\\ l\in\mathcal{M}_f/\{i\}}}p^f_{l,n} +\left|h^f_{i,n}\right|^2\left|h^f_{e,n}\right|^2\sum_{l\in\mathcal{M}_f/\{i\}}p^f_{l,n}, \tag{58}$$

where $\hat{I}^f_{m,n}=\sum_{f'\in\mathcal{F}/f}\left|h^{f'}_{m,n}\right|^2\sum_{i\in\mathcal{M}_{f'}}p^{f'}_{i,n}$ and $\hat{I}^f_{e,n}=\sum_{f'\in\mathcal{F}/f}\left|h^{f'}_{e,n}\right|^2\sum_{i\in\mathcal{M}_{f'}}p^{f'}_{i,n}$. Moreover, $\tilde{r}^f_{m,n}$ is defined as:

$$\tilde{r}^f_{m,n}=\log\left(1+\frac{p^f_{m,n}\left|h^f_{m,n}\right|^2}{\left|h^f_{m,n}\right|^2\sum_{\substack{|h^f_{m,n}|^2\le|h^f_{i,n}|^2\\ i\in\mathcal{M}_f/\{m\}}}p^f_{i,n}+\hat{I}^f_{m,n}+\sigma^2}\right), \tag{59}$$

B. MONOTONIC OPTIMIZATION

In the second step, our aim is to formulate the optimization problem (56) as a monotonic optimization problem in the canonical form. As we know, the optimization problem (56) is a non-monotonic problem because the objective function is not increasing function and constraints (56d), (56e), and (56f) are not inside normal or conormal sets. Since the optimization problem is a problem with hidden monotonicity [34], we can rewrite the objective function and non-monotonic constraints to a differences of increasing function form. Hence, let us reformulate the objective function as $\tilde{r}^f_{m,n}-\upsilon^f_{m,n}=g^{f+}_{m,n}-g^{f-}_{m,n}$ where $g^{f+}_{m,n}=\log\left(\left|h^f_{m,n}\right|^2\sum_{\substack{|h^f_{m,n}|^2\le|h^f_{i,n}|^2\\ i\in\mathcal{M}_f/\{m\}}}p^f_{i,n}+\hat{I}^f_{m,n}+\sigma^2+p^f_{m,n}\left|h^f_{m,n}\right|^2\right)$ and

$$g^{f-}_{m,n}=\log\left(\left|h^f_{m,n}\right|^2\sum_{\substack{|h^f_{m,n}|^2\le|h^f_{i,n}|^2\\ i\in\mathcal{M}_f/\{m\}}}p^f_{i,n}+\hat{I}^f_{m,n}+\sigma^2\right)+\upsilon^f_{m,n}.$$

We introduce auxiliary variables T_1, T_2, T_3, T_4, and T_5 to reformulate (56) as [54], [55]:

$$\max_{\mathbf{P},\boldsymbol{\upsilon},T_1,T_2,T_3,T_4,T_5}\sum_{\forall f\in\mathcal{F}}\sum_{\forall m\in\mathcal{M}_f}\sum_{\forall n\in\mathcal{N}}\left\{g^{f+}_{m,n}+T^f_{4,m,n}\right\}, \tag{60a}$$

$$\text{s.t.:}\quad (56b), (56c), (56g), \tag{60b}$$

$$O^+(\mathbf{P})+T^f_{1,m,i,n}\le O^+\left(\mathbf{P}^{\text{mask}}\right),\quad \forall f\in\mathcal{F}, \tag{60c}$$
$$n\in\mathcal{N},\quad m,i\in\mathcal{M}_f,\ |h^f_{i,n}|^2\le|h^f_{m,n}|^2,\ i\neq m,$$

$$O^-(\mathbf{P})+T^f_{1,m,i,n}\ge O^+\left(\mathbf{P}^{\text{mask}}\right),\quad \forall f\in\mathcal{F}, \tag{60d}$$
$$n\in\mathcal{N},\quad m,i\in\mathcal{M}_f,\ |h^f_{i,n}|^2\le|h^f_{m,n}|^2,\ i\neq m,$$

$$0\le T^f_{1,m,i,n}\le O^+\left(\mathbf{P}^{\text{mask}}\right)-O^+(0),\quad \forall f\in\mathcal{F}, \tag{60e}$$
$$n\in\mathcal{N},\quad m,i\in\mathcal{M}_f,\ |h^f_{i,n}|^2\le|h^f_{m,n}|^2,\ i\neq m,$$

$$\hat{O}^+(\mathbf{P})+T^f_{2,m,i,n,e}\le\hat{O}^+\left(\mathbf{P}^{\text{mask}}\right),\quad \forall f\in\mathcal{F}, \tag{60f}$$

$$n \in \mathcal{N}, \quad m, i \in \mathcal{M}_f, \ e \in \mathcal{E}, \ |h^f_{i,n}|^2 \leq |h^f_{e,n}|^2,$$
$$\hat{O}^-(\mathbf{P}) + T^f_{2,m,i,n,e} \geq \hat{O}^+\left(\mathbf{P}^{\text{mask}}\right), \quad \forall f \in \mathcal{F}, \tag{60g}$$
$$n \in \mathcal{N}, \quad m, i \in \mathcal{M}_f, \ e \in \mathcal{E}, \ |h^f_{i,n}|^2 \leq |h^f_{e,n}|^2,$$
$$0 \leq T^f_{2,m,i,n,e} \leq \hat{O}^+\left(\mathbf{P}^{\text{mask}}\right) - \hat{O}^+(0), \quad \forall f \in \mathcal{F}, \tag{60h}$$
$$n \in \mathcal{N}, \quad m, i \in \mathcal{M}_f, \ e \in \mathcal{E}, \ |h^f_{i,n}|^2 \leq |h^f_{e,n}|^2,$$
$$\tilde{O}^+(\mathbf{P}) + T^f_{3,m,n,e} \leq \tilde{O}^+\left(\mathbf{P}^{\text{mask}}\right), \quad \forall e \in \mathcal{E}, \tag{60i}$$
$$n \in \mathcal{N}, \quad f \in \mathcal{F}, \ m \in \mathcal{M}_f,$$
$$\tilde{O}^-(\mathbf{P}) + T^f_{3,m,n,e} \geq \tilde{O}^+\left(\mathbf{P}^{\text{mask}}\right), \quad \forall e \in \mathcal{E}, \tag{60j}$$
$$n \in \mathcal{N}, \quad f \in \mathcal{F}, \ m \in \mathcal{M}_f,$$
$$0 \leq T^f_{3,m,n,e} \leq \tilde{O}^+\left(\mathbf{P}^{\text{mask}}\right) - \tilde{O}^+(0), \quad \forall e \in \mathcal{E}, \tag{60k}$$
$$n \in \mathcal{N}, \quad f \in \mathcal{F}, \ m \in \mathcal{M}_f,$$
$$T^f_{4,m,n} + g^{f-}_{m,n}(\mathbf{P}) \leq g^{f-}_{m,n}\left(\mathbf{P}^{\text{mask}}\right) \tag{60l}$$
$$0 \leq T^f_{4,m,n} \leq g^{f-}_{m,n}\left(\mathbf{P}^{\text{mask}}\right) - g^{f-}_{m,n}(0) \tag{60m}$$
$$g^{f-}_{m,n}(\mathbf{P}) + T^f_{5,m,n} \leq g^{f-}_{m,n}\left(\mathbf{P}^{\text{mask}}\right), \quad \forall n \in \mathcal{N}, \tag{60n}$$
$$f \in \mathcal{F}, m \in \mathcal{M}_f,$$
$$g^{f+}_{m,n}(\mathbf{P}) + T^f_{5,m,n} \geq g^{f-}_{m,n}\left(\mathbf{P}^{\text{mask}}\right), \quad \forall n \in \mathcal{N}, \tag{60o}$$
$$f \in \mathcal{F}, \forall m \in \mathcal{M}_f,$$
$$0 \leq T^f_{5,m,n} \leq g^{f-}_{m,n}\left(\mathbf{P}^{\text{mask}}\right) - g^{f-}_{m,n}(0), \quad \forall n \in \mathcal{N}, \tag{60p}$$
$$f \in \mathcal{F}, \quad m \in \mathcal{M}_f,$$

where, $\mathbf{P}^{\text{mask}}$ is a vector which is defined as $\mathbf{P}^{\text{mask}} = \left[p^{f,\text{mask}}_{m,n}\right], \forall m \in \mathcal{M}_f, n \in \mathcal{N}, f \in \mathcal{F}$, where $p^{f,\text{mask}}_{m,n}$ is the transmit power spectral mask for user m on the n^{th} subcarrier, which is served by the f^{th} BS. Moreover, $O^+(\mathbf{P}) = p^f_{m,n}p^f_{i,n}(|h^f_{i,n}|^2\sigma^2 + \left|h^f_{i,n}\right|^2\left|h^f_{m,n}\right|^2 \sum_{\substack{\left|h^f_{m,n}\right|^2 \leq \left|h^f_{l,n}\right|^2 \\ l \in \mathcal{M}_f/\{i\}}} p^f_{l,n} + h^f_{i,n}\hat{I}^f_{m,n})$, $O^-(\mathbf{P}) = p^f_{m,n}p^f_{i,n}(|h^f_{m,n}|^2\sigma^2 + h^f_{m,n}\hat{I}^f_{i,n} + \left|h^f_{m,n}\right|^2\left|h^f_{i,n}\right|^2 \sum_{\substack{\left|h^f_{i,n}\right|^2 \leq \left|h^f_{l,n}\right|^2 \\ l \in \mathcal{M}_f/\{i\}}} p^f_{l,n})$, $\hat{O}^+(\mathbf{P}) = p^f_{m,n}p^f_{i,n}(|h^f_{e,n}|^2\sigma^2 + h^f_{e,n}\hat{I}^f_{i,n} + \left|h^f_{e,n}\right|^2\left|h^f_{i,n}\right|^2 \sum_{\substack{\left|h^f_{i,n}\right|^2 \leq \left|h^f_{l,n}\right|^2 \\ l \in \mathcal{M}_f/\{i\}}} p^f_{l,n})$, $\hat{O}^-(\mathbf{P}) = p^f_{m,n}p^f_{i,n}(|h^f_{i,n}|^2\sigma^2 + h^f_{i,n}\hat{I}^f_{e,n} + \left|h^f_{i,n}\right|^2\left|h^f_{e,n}\right|^2 \sum_{l \in \mathcal{M}_f/\{i\}} p^f_{l,n},)$, $\tilde{O}^+(\mathbf{P}) = \log(\left|h^f_{e,n}\right|^2 \sum_{i \in \mathcal{M}_f/\{m\}} p^f_{i,n} + \hat{I}^f_{e,n} + \sigma^2 + p^f_{m,n}\left|h^f_{e,n}\right|^2)$, and $\tilde{O}^-(\mathbf{P}) = \log(\left|h^f_{e,n}\right|^2 \sum_{i \in \mathcal{M}_f/\{m\}} p^f_{i,n} + \hat{I}^f_{e,n} + \sigma^2) + \upsilon^f_{m,n}$. According to problem (60), we define two sets as follows:

$$\aleph_1 = \Big\{(\mathbf{P}, \boldsymbol{\upsilon}, T_1, T_2, T_3, T_4, T_5) : \mathbf{P} \preceq \mathbf{P}^{\text{mask}}, \text{(56b)}, \text{(56g)}, \times \text{(60c)}, \text{(60f)}, \text{(60i)}, \text{(60l)}, \text{(60n)}\Big\}, \tag{61}$$

and

$$\aleph_2 = \{(\mathbf{P}, \boldsymbol{\upsilon}, T_1, T_2, T_3, T_4, T_5) : \mathbf{P} \succeq 0, \text{(56c)}, \text{(60d)}, \text{(60g)}, \text{(60j)}, \text{(60m)}, \text{(60o)}\}, \tag{62}$$

in fact, the intersection of sets $\aleph_1$ and $\aleph_2$ is the feasible set of problem (60), moreover, $\aleph_1$ and $\aleph_2$ are normal and co-normal sets, respectively, in the following hyper-rectangle, [54], [55]:

$$\left[0, \mathbf{P}^{\text{mask}}\right] \times \left[0, O^+\left(\mathbf{P}^{\text{mask}}\right) - O^+(0)\right] \times \left[0, \hat{O}^+\left(\mathbf{P}^{\text{mask}}\right) - \hat{O}^+(0)\right] \times \left[0, \tilde{O}^+\left(\mathbf{P}^{\text{mask}}\right) - \tilde{O}^+(0)\right] \times \left[0, g^{f-}_{m,n}\left(\mathbf{P}^{\text{mask}}\right) - g^{f-}_{m,n}(0)\right] \times \left[0, \boldsymbol{\upsilon}^{\max}\right]. \tag{63}$$

finally, problem (60) is a monotonic problem in a canonical form, based on Definition 5 in [55]. Hence, the optimization problem (60) can be solved by using the polyblock algorithm. As mentioned way, at which we convert (17) to a canonical form of monotonic optimization, we can convert (53) to a canonical form.

C. COMPUTATIONAL COMPLEXITY

In this section we discuss about the computational complexity of the polyblock algorithm. As we know, the computational complexity of this algorithm depends on the number of variables and form of the functions in the optimization problem. In the polyplock algorithm four main steps are performed. In the first step, the best vertex should be found, in the second step we find projection of the selected vertex, improper vertexes are removed in the third step, and new vertex set is found in the fourth step. The dimension of our optimization problem is $\Im_0 = F + NF(3M + 1) + (M - 1)(M(M - 2) + 3NFM + 3NFME) + 3FNME)$, the convergence of algorithm for stopping threshold 10^{-3}, occurs approximately after $\Im_1 = 10^4$ iterations, the bisection algorithm which gives projection of vertex, with stopping threshold 10^{-3}, has $\Im_2 = 10^3$ iterations, approximately. Hence, the complexity order can be written as $O(\Im_1(\Im_1 \times \Im_0 + \Im_2))$, [12].

In order to present a comprehensive comparison between the optimal solution (monotonic) and the suboptimal solution (the proposed solution), we provided Table 2. As mentioned, in the optimal solution, first we convert the optimization problems to the canonical form of monotonic

$$\gamma_{m,n}^{f}=\frac{p_{m,n}^{f}\left\|h_{m,n}^{f}w_{m,n}^{f\dagger}\right\|^{2}}{I_{m,n}^{f}+\sum_{\substack{\left\|h_{m,n}^{f}\right\|^{2}\leq\left\|h_{i,n}^{f}\right\|^{2}\\ \times i\in\mathcal{M}_f/\{m\}}}\left\|h_{m,n}^{f}w_{i,n}^{f\dagger}\right\|^{2}p_{i,n}^{f}\rho_{i,n}^{f}+\sigma^{2}}, \tag{66}$$

optimization problem and finally, we solve them by employing the Polyblock algorithm. However, in the suboptimal solution, first convert the optimization problems to two subproblems, power and subcarrier allocation, and solve them separately, and finally, we solve the power allocation with the successive convex approximation method and subcarrier allocation with the mesh adaptive direct search algorithm. Furthermore, the performance of the optimal solution with respect to the suboptimal solution is approximately 13.05% while its complexity with respect to the suboptimal solution is approximately 1.3772×10^4 times. This illustrates which the complexity of optimal solution is highly significant compared to the performance increase. Note that, the global optimal solution is only considered as a benchmark for the optimality gap analysis.

VII. MULTIPLE ANTENNAS BSS SCENARIO

In this section, our aim is to evaluate SIC avoidance when the BSs are equipped with K_T antennas. BS f transmits $\sum_{j=1}^{M_f}\sqrt{p_{j,n}^{f}}\rho_{j,n}^{f}w_{j,n}^{f}s_{j,n}^{f}$ on subcarrier n, where $w_{m,n}^{f}$ is precoding vector, $w_{m,n}^{f}\in\mathcal{C}^{K_T\times 1}$. The received signals on the m^{th} user and the e^{th} adversary, that are located in the coverage region of BS f, on the n^{th} subcarrier are expressed as

$$y_{m,n}^{f}=\sum_{i\in\mathcal{M}_f}\sqrt{p_{i,n}^{f}}\rho_{i,n}^{f}h_{m,n}^{f\dagger}w_{i,n}^{f}s_{i,n}^{f} + \sum_{f'\in\mathcal{F}/f}\sum_{i\in\mathcal{M}_{f'}}\sqrt{p_{i,n}^{f'}}\rho_{i,n}^{f'}h_{m,n}^{f'\dagger}w_{i,n}^{f'}s_{i,n}^{f'}+Z_{m,n}^{f}, \tag{64}$$

$$y_{e,n}^{f}=\sum_{i\in\mathcal{M}_f}p_{i,n}^{f}\rho_{i,n}^{f}h_{e,n}^{f\dagger}w_{i,n}^{f}s_{i,n}^{f} + \sum_{f'\in\mathcal{F}/f}\sum_{i\in\mathcal{M}_{f'}}p_{i,n}^{f'}\rho_{i,n}^{f'}h_{e,n}^{f'\dagger}w_{i,n}^{f'}s_{i,n}^{f'}+Z_{e,n}^{f}, \tag{65}$$

respectively. where $\dagger$ is the hermitian operator and $h_{m,n}^{f}\in\mathcal{C}^{K_T\times 1}$. We assume the BSs employ Maximum Ratio Transmission technique (MRT), hence, $w_{m,n}^{f}=h_{m,n}^{f}/\left\|h_{m,n}^{f}\right\|$. When user m applies SIC, its SINR in BS f on subcarrier n can be expressed as (66), as shown at the top of this page, where $I_{m,n}^{f}=\sum_{f'\in F/f}\sum_{i\in M_{f'}}p_{i,n}^{f'}\rho_{i,n}^{f'}\left\|h_{m,n}^{f'}w_{i,n}^{f'\dagger}\right\|^{2}$. SINR of the eavesdropper e in BS f on subcarrier n can be obtained as:

$$\gamma_{e,n}^{f,m}=\frac{p_{m,n}^{f}\left\|h_{e,n}^{f}w_{m,n}^{f\dagger}\right\|^{2}}{\sum_{i\in\mathcal{M}_f/\{m\}}\left\|h_{e,n}^{f}w_{i,n}^{f\dagger}\right\|^{2}p_{i,n}^{f}\rho_{i,n}^{f}+I_{e,n}^{f}+\sigma^{2}}, \tag{67}$$

where $I_{e,n}^{f}=\sum_{f'\in F/f}\sum_{i\in M_{f'}}p_{i,n}^{f'}\rho_{i,n}^{f'}\left\|h_{e,n}^{f'}w_{i,n}^{f'\dagger}\right\|^{2}$. The optimization problem can be written as follows:

$$\max_{\mathbf{P},\boldsymbol{\rho}}\sum_{\forall f\in\mathcal{F}}\sum_{\forall m\in\mathcal{M}_f}\sum_{\forall n\in\mathcal{N}}\rho_{m,n}^{f}\left\{r_{m,n}^{f}-r_{e_{\max},n}^{f,m}\right\}, \tag{68a}$$

$$\text{s.t.}: C_1: \quad (13b), (13c), (14), (14)$$

$$C_2: \quad \rho_{m,n}^{f}\rho_{i,n}^{f}Q_{m,i,n}^{f}(\boldsymbol{\rho},\mathbf{P})\leq 0, \quad \forall f\in\mathcal{F}, \quad n\in\mathcal{N}, \quad m,i\in\mathcal{M}_f, \quad \left\|h_{i,n}^{f}\right\|^{2}\leq\left\|h_{m,n}^{f}\right\|^{2}, \quad i\neq m, \tag{68b}$$

$$C_3: \quad \rho_{m,n}^{f}\rho_{i,n}^{f}\psi_{m,i,n,e}^{f}(\boldsymbol{\rho},\mathbf{P})\geq 0, \quad \forall f\in\mathcal{F}, \quad n\in\mathcal{N}, \quad m,i\in\mathcal{M}_f, \quad e\in\mathcal{E}, \quad \left\|h_{i,n}^{f}\right\|^{2}\leq\left\|h_{e,n}^{f}\right\|^{2}, \tag{68c}$$

$$C_4: \quad r_{m,n}^{f}-r_{e_{\max},n}^{f,m}\geq 0, \quad \forall m\in\mathcal{M}_f, \ n\in\mathcal{N}, \ f\in\mathcal{F}, \tag{68d}$$

where $Q_{m,i,n}^{f}$ and $\psi_{m,i,n}^{f}$ can be obtained similar to inequalities (5) and (9), respectively. In order to solve the optimization problem (68), we employ an iteration algorithm similar to SISO scenario, i.e., Algorithm 1.

VIII. SIMULATION RESULTS

In this section, we provide numerical results to evaluate the performance of the proposed scheme. The simulation parameters are considered as: $p_0^{\max}=16$ dB (maximum allowable transmit power of MBS), $p_m^{\max}=6$ dB, $\forall m\in\mathcal{M}/\{1\}$ (maximum allowable transmit power of SBS), Power Spectral Density (PSD) of noise is -130 dBm/Hz, $\alpha=4$. Maximum coverage MBS and SBS are supposed 1500 m and 15 m, respectively.

At the first glance, it may seem that condition (9) can not be satisfied through the proposed resource allocation algorithm. Hence, we plot Fig. 2 which illustrates the outage probability of condition (9) versus the number of subcarriers to show condition (9) are satisfied through the proposed resource allocation algorithm. Condition (9) can be in outage if it cannot be satisfied with optimal optimization variables. As seen in

TABLE 2. The comparison of the optimal and suboptimal solutions.

Items	The optimal solution	The suboptimal solution	The optimal over the suboptimal solution
Used approach	With out loss generality, the optimization problems are converted to the canonical form of monotonic optimization problem	The optimization problems are converted to two subproblems, power and subcarrier allocation and are solved separately.	
Used methods/ algorithm	Polyblock algorithm	Power allocation with the successive convex approximation method, subcarrier allocation with the mesh adaptive direct search algorithm are solved.	
Performance	126.8 (Bits/Sec/Hz)	110.11 (Bits/Sec/Hz)	13.05%
Complexity	$O(\Im_1(\Im_1 \times (F+NF(3M+1)+(M-1)(M(M-2)+3NFM+3NFME)+3FNME)+\Im_2))$	$O\left(\frac{\log\left(\frac{F(1+N(1+M+M(M-1)+ME(M-1)+ME))}{t\partial}\right)}{\log(\xi)}\right)$	1.3772×10^4 times

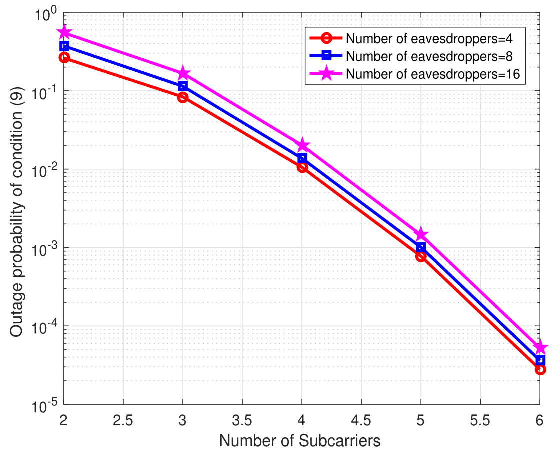

FIGURE 2. The outage probability of condition (9) versus the number of subcarriers.

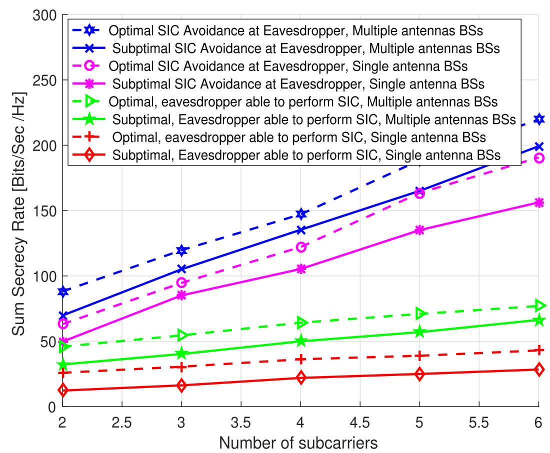

FIGURE 3. Secrecy sum rate versus the number of subcarriers, comparison between the proposed scheme (SIC avoidance at the eavesdroppers) and when the eavesdropper can do SIC, $M = 3$ per km^2, $E = 2$ per km^2, $F = 2$ per km^2, and $M_t = 8$.

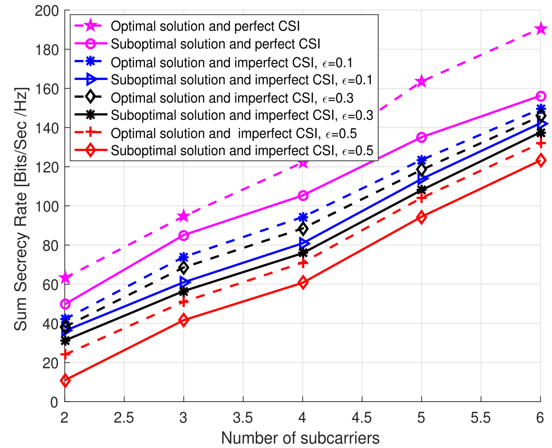

FIGURE 4. Secrecy sum rate versus the number of subcarriers for perfect and imperfect CSI in the proposed scheme, $F = 2$ per km^2, $M = 3$ per km^2, $E = 2$ per km^2.

this figure, by increasing the number of subcarriers the outage probability of condition (9) decreases.

In Fig. 3, the sum secrecy rate versus the number of subcarriers is shown. Also this figure compares our proposed scheme at which the eavesdroppers are not able to perform SIC with the case they can perform SIC. As seen in this figure, the sum secrecy rate in our proposed scheme has 72% gap with the conventional type, because in the proposed scheme we do not allow eavesdroppers to perform SIC, even if they know the channel ordering, but in the conventional type the eavesdroppers can perform SIC. Moreover, this figure compares single and multiple antennas Bss scenarios and shows when the BSs are equipped with multiple antennas the secrecy rate increases.

In Fig. 4, we compare the performance of the proposed scheme for the perfect and imperfect CSI scenarios. Moreover, this figure shows imperfect CSI sensitivity with respect to the upper bound of error. As seen, when $\epsilon = \epsilon_e = \epsilon_m = 0.1$, the imperfect SCI scenario has 20.7% gap with respect to perfect CSI. By increasing ϵ to 0.3 and 0.5, this gap is increased to 26.14% and 44.53%, respectively.

Fig. 5, shows the sum secrecy rate versus the number of eavesdroppers. As seen, with increasing the number of eavesdroppers in our system model, the sum secrecy rate is decreased. This is because, as we know, it is assumed the eavesdroppers are non-clutsions, therefore, when an eaves-

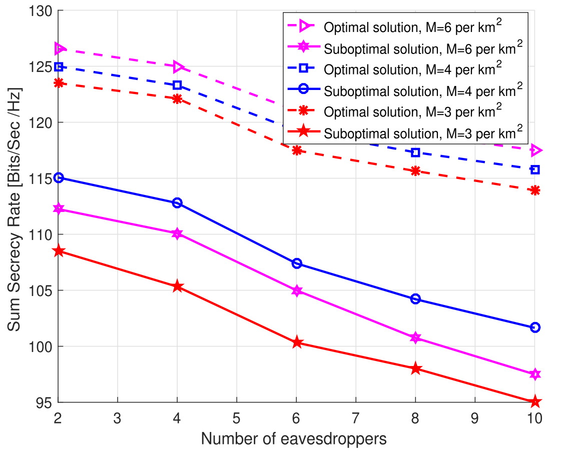

FIGURE 5. Secrecy sum rate versus the number of eavesdroppers, in the proposed scheme, $F = 2$ per km^2, $N = 4$, $E = 2$ per km^2.

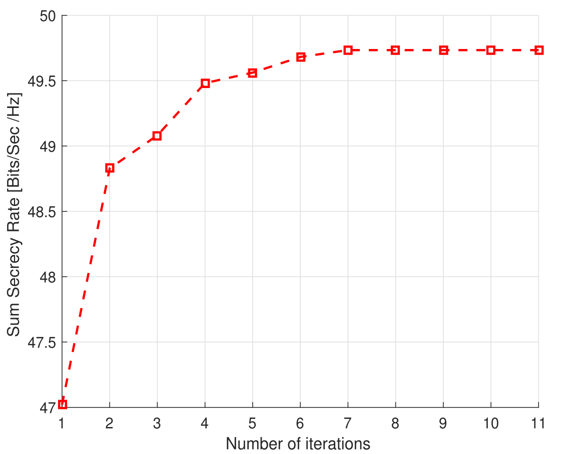

FIGURE 6. Convergence of the proposed algorithm.

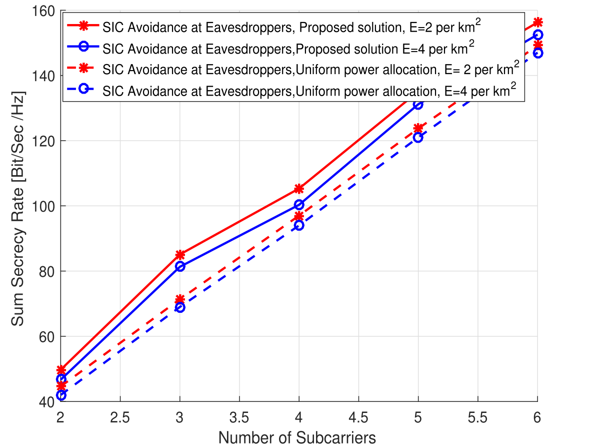

FIGURE 7. Comparison between our proposed solution and the uniform power allocation method, $M = 3$ per km^2, F = 2 per km^2.

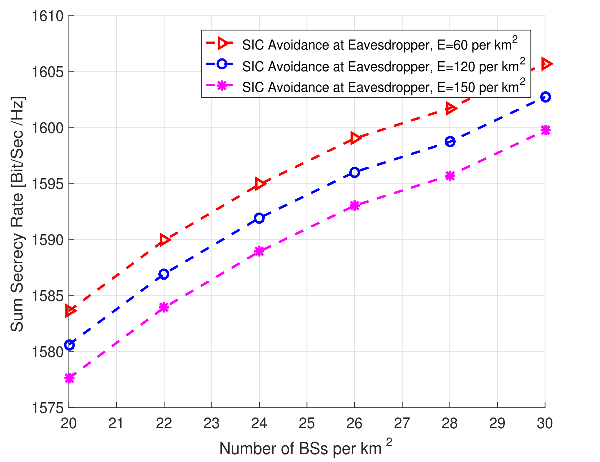

FIGURE 8. Secrecy sum rate versus the number of BSs in HUDN, $N = 48$, $M = 300$ per km^2.

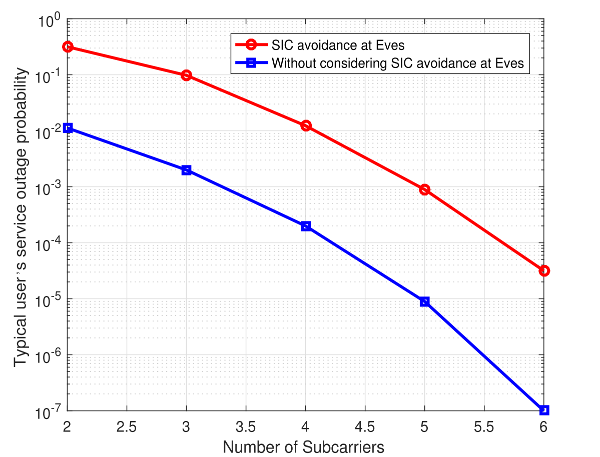

FIGURE 9. Typical user's service outage probability versus the number of subcarriers.

dropper is added to the system, its channel maybe better than others, hence the secrecy rate changes (decreases). In the simulation, we use the Monte Carlo method, therefore when the number of eavesdroppers is increased, the secrecy rate decreases on average.

Fig. 6 presents the convergence behavior of the proposed algorithm. We observe that the algorithm converges in iteration 8, in ASM, approximately. In this figure, we assume $E = 2$ per km^2, $F = 2$ per km^2, $M = 3$ per km^2, and $N = 2$.

In addition, we show optimal solution in all of these figures. As seen, the proposed suboptimal solution which has low complexity with respect to the monotonic optimization problem, is closed to the optimal solution, for example in Fig. 5, the optimal solution has approximately 13.05% gap with the proposed suboptimal solution.

As mentioned in Section V, for evaluating the performance degradation due to the uniform power allocation, we compare the uniform power allocation method for a small network dimension with our proposed solution i.e., joint power and subcarrier allocation in Fig. 7. As shown in this figure, there is approximately 9% performance gap between these methods.

In Fig. 8, sum secrecy rate versus the number of BSs in HUDN for massive connectivity is evaluated. Besides, this figure investigates effect of number of eavesdroppers in massive connectivity. As seen, by increasing one BS per Km^2, the sum secrecy rate 2.5 unit increases, approximately.

Fig. 9 illustrates the typical user's service outage probability versus the number of subcarriers in two cases 1) SIC avoidance at eavesdroppers (the proposed scheme), 2) without considering SIC avoidance at eavesdroppers (conventional scheme). The typical user's service can be in outage if the constraints related to the typical user is satisfied with $\rho = 0$ which leads to that the typical user's secrecy rate is 0. As seen in this figure, by increasing the number of subcarriers the typical user's service outage probability decreases. It is necessary to mention that although service outage probability in the case of "without considering SIC avoidance at eavesdroppers" is less than case of "SIC avoidance at eavesdroppers", as seen in Fig. 3, the ergodic sum secrecy rate in our proposed scheme has 72% gap with the conventional type.

IX. CONCLUSION

In this paper, we investigated PLS for power domain non-orthogonal multiple access based HetNet. We proposed a novel resource allocation to maximize the sum secrecy rate in PD-NOMA based HetNet. In the proposed scenario, the eavesdroppers are not allowed to perform successive interference cancellation, but the legitimate users are able to perform it. Hence, all users' signals in the eavesdroppers are treated as interference, while some users' signals can be canceled in the desired users, therefore, less interference is experienced by users. In order to solve the optimization problem, we adopted the iterative algorithm called ASM, i.e., to convert the optimization problems to two subproblems power and subcarrier allocation and solve them alternatively. In each iteration of ASM, we consider fixed subcarrier and allocated power, then, for subcarrier allocation we consider fixed power. In each iteration of this method, power allocation problem, is non-convex and subcarrier allocation is NLP. Hence, we solve the power allocation by the SCA approach. To this end, we use the DC approximation, to transform the non-convex problem into canonical form of convex optimization. Also, we solve subcarrier allocation, by exploiting MADS, hence we employ the existing solver called NOMAD. Moreover, we obtained optimal solution and the optimality gap of the proposed solution method, by converting the optimization problems to a canonical form of the monotonic optimization problem and exploiting the polyblock algorithm. Besides, we evaluated the proposed scheme for secure massive connectivity in mMTC cases in HUDNs. As resource allocation in this networks has high dimension complexity, we allocated the transmit power uniformly to users and showed the performance of uniform power allocation is close to the performance of our proposed solution. Furthermore, we investigated multiple antennas base stations scenario in this literature. Numerical results show the sum secrecy rate in our novel resource allocation has 72% gap with the conventional type at which the eavesdroppers are able to perform SIC. Moreover, we investigated imperfect CSI of the eavesdroppers scenario and compared it with the perfect CSI case. It is necessary to mention that we investigate and analyze to find a low complex and optimal solution for the proposed optimization problem as future work.

APPENDIX

In the SCA approach with the DC approximation, a sequence of improved feasible solutions is generated and is converged to a local optimum, [47].

Proof: As mentioned, we approximate (37) with function (38). Gradient of function $H^f_{m,n}(\mathbf{P})$ is its super gradient, because $H^f_{m,n}(\mathbf{P})$ is a concave function [53]

. Hence, we have

$$H^f_{m,n}(\mathbf{P}(\mu)) \leq H^f_{m,n}(\mathbf{P}(\mu-1)) + \nabla^T H^f_{m,n}(\mathbf{P}(\mu-1))(\mathbf{P}(\mu)-\mathbf{P}(\mu-1)), \tag{69}$$

Therefore, in the objective function, we have:

$$\begin{aligned}
&\sum_{\forall f\in\mathcal{F}}\sum_{\forall m\in\mathcal{M}_f}\sum_{\forall n\in\mathcal{N}_f}\rho^f_{m,n}\left\{G^f_{m,n}(\mathbf{P}(\mu)) - H^f_{m,n}(\mathbf{P}(\mu))\right\}\\
&\geq \sum_{\forall f\in F}\sum_{\forall m\in M_f}\sum_{\forall n\in N_f}\rho^f_{m,n}\Big\{G^f_{m,n}(\mathbf{P}(\mu)) - H^f_{m,n}(\mathbf{P}(\mu-1))\\
&\quad - \nabla^T H^f_{m,n}(\mathbf{P}(\mu-1))(\mathbf{P}(\mu)-\mathbf{P}(\mu-1))\Big\}\\
&= \max_{\mathbf{P}}\sum_{\forall f\in F}\sum_{\forall m\in M_f}\sum_{\forall n\in N_f}\rho^f_{m,n}\Big\{G^f_{m,n}(\mathbf{P})\\
&\quad -H^f_{m,n}(\mathbf{P}(\mu-1)) - \nabla^T H^f_{m,n}(\mathbf{P}(\mu-1))(\mathbf{P}-\mathbf{P}(\mu-1))\Big\}\\
&\geq \sum_{\forall f\in F}\sum_{\forall m\in M_f}\sum_{\forall n\in N_f}\rho^f_{m,n}\Big\{G^f_{m,n}(\mathbf{P}(\mu-1))\\
&\quad - H^f_{m,n}(\mathbf{P}(\mu-1)) - \nabla^T H^f_{m,n}(\mathbf{P}(\mu-1))\\
&\quad \times(\mathbf{P}(\mu-1)-\mathbf{P}(\mu-1))\}\\
&= \sum_{\forall f\in\mathcal{F}}\sum_{\forall m\in\mathcal{M}_f}\sum_{\forall n\in\mathcal{N}_f}\rho^f_{m,n}\\
&\quad \times\left\{G^f_{m,n}(\mathbf{P}(\mu-1)) - H^f_{m,n}(\mathbf{P}(\mu-1))\right\}.
\end{aligned}$$

Therefore, after iteration μ, the objective function value either increases or stays unchanged with respect to iteration $\mu - 1$.

REFERENCES

[1] *IMT Vision–Framework and Overall Objectives of the Future Development of IMT for 2020 and Beyond*, document ITU-R M.2083-0, Sep. 2015.
[2] J. Zhu, Y. Song, D. Jiang, and H. Song, "A new deep-q-learning-based transmission scheduling mechanism for the cognitive Internet of Things," *IEEE Internet Things J.*, vol. 5, no. 4, pp. 2375–2385, Aug. 2018.
[3] Z. Qin, X. Yue, Y. Liu, Z. Ding, and A. Nallanathan, "User association and resource allocation in unified non-orthogonal multiple access enabled heterogeneous ultra dense networks," *IEEE Commun. Mag.*, vol. 56, no. 6, pp. 86–92, Jun. 2018.
[4] Y. Saito, A. Benjebbour, Y. Kishiyama, and T. Nakamura, "System-level performance evaluation of downlink non-orthogonal multiple access (NOMA)," in *Proc. IEEE Annu. Symp. PIMRC*, London, U.K., Sep. 2013, pp. 611–615.
[5] M. Al-Imari, P. Xiao, M. A. Imran, and R. Tafazolli, "Uplink non-orthogonal multiple access for 5G wireless networks," in *Proc. ISWCS*, Barcelona, Spain, Aug. 2014, pp. 781–785.

[6] T. M. Cover and J. A. Thomas, *Elements of Information Theory*. New York, NY, USA: Wiley, 1991.

[7] T. Cover, "Broadcast channels," *IEEE Trans. Inf. Theory*, vol. 18, no. 1, pp. 2–14, Jan. 1972.

[8] J. G. Andrews, "Interference cancellation for cellular systems: A contemporary overview," *IEEE Trans. Wireless Commun.*, vol. 12, no. 2, pp. 19–29, Apr. 2005.

[9] Z. Ding, Z. Yang, P. Fan, and H. V. Poor, "On the performance of non-orthogonal multiple access in 5G systems with randomly deployed users," *IEEE Signal Process. Lett.*, vol. 21, no. 12, pp. 1501–1505, Dec. 2014.

[10] J. Wang, B. Xia, K. Xiao, Y. Gao, and S. Ma, "Outage performance analysis for wireless non-orthogonal multiple access systems," *IEEE Access*, vol. 6, pp. 3611–3618, Jan. 2018.

[11] Z. Xiao, L. Zhu, J. Choi, P. Xia, and X.-G. Xia, "Joint power allocation and beamforming for non-orthogonal multiple access (NOMA) in 5G millimeter wave communications," *IEEE Trans. Wireless Commun.*, vol. 17, no. 5, pp. 2961–2974, May 2018.

[12] M. Moltafet, P. Azmi, N. Mokari, M. R. Javan, and A. Mokdad, "Optimal and fair energy efficient resource allocation for energy harvesting-enabled-PD-NOMA-based HetNets," *IEEE Trans. Wireless Commun.*, vol. 17, no. 3, pp. 2054–2067, Mar. 2018.

[13] L. Dai, B. Wang, Y. Yuan, S. Han, C.-L. I, and Z. Wang, "Non-orthogonal multiple access for 5G: Solutions, challenges, opportunities, and future research trends," *IEEE Commun. Mag.*, vol. 53, no. 9, pp. 74–81, Sep. 2015.

[14] Y. Saito, Y. Kishiyama, A. Benjebbour, T. Nakamura, A. Li, and K. Higuchi, "Non-orthogonal multiple access (NOMA) for cellular future radio access," in *Proc. IEEE 77th Veh. Technol. Conf.*, Dresden, Germany, Jun. 2013, pp. 1–5.

[15] Z. Ding, Y. Liu, J. Choi, Q. Sun, M. Elkashlan, C.-L. I, and H. V. Poor, "Application of non-orthogonal multiple access in LTE and 5G networks," *IEEE Commun. Mag.*, vol. 55, no. 2, pp. 185–191, Feb. 2017.

[16] A. D. Wyner, "The wire-tap channel," *Bell Syst. Tech. J.*, vol. 54, no. 8, pp. 1355–1387, 1975.

[17] J. Granjal, E. Monteiro, and J. S. Silva, "Security for the Internet of Things: A survey of existing protocols and open research issues," *IEEE Commun. Surveys Tuts.*, vol. 17, no. 3, pp. 1294–1312, 3rd Quart., 2015.

[18] N. Yang, L. Wang, G. Geraci, M. Elkashlan, J. Yuan, and M. Di Renzo, "Safeguarding 5G wireless communication networks using physical layer security," *IEEE Commun. Mag.*, vol. 53, no. 4, pp. 20–27, Apr. 2015.

[19] Y. Zhang, H.-M. Wang, Q. Yang, and Z. Ding, "Secrecy sum rate maximization in non-orthogonal multiple access," *IEEE Commun. Lett.*, vol. 20, no. 5, pp. 930–933, May 2016.

[20] L. Lv, Z. Ding, Q. Ni, and J. Chen, "Secure MISO-NOMA transmission with artificial noise," *IEEE Trans. Veh. Technol.*, vol. 67, no. 7, pp. 6700–6705, Jul. 2018.

[21] G. He, L. Li, X. Li, W. Chen, L.-L. Yang, and Z. Han, "Secrecy sum rate maximization in NOMA systems with wireless information and power transfer," in *Proc. 9th Int. Conf. Wireless Commun. Signal Process.*, Nanjing, China, Oct. 2017, pp. 1-6.

[22] H. Lei, J. Zhang, K.-H. Park, P. Xu, I. S. Ansari, G. Pan, B. Alomair, and M.-S. Alouini, "On secure NOMA systems with transmit antenna selection schemes," *IEEE Access*, vol. 5, pp. 17450–17464, 2017.

[23] Z. Xiang, W. Yang, Y. Cai, Y. Cheng, H. Wu, and M. Wang, "Secrecy performance analysis of uplink NOMA in IoT networks," in *Proc. IEEE/CIC Int. Conf. Commun. China*, Beijing, China, Aug. 2018, pp. 506–510.

[24] Y. Liu, Z. Qin, M. Elkashlan, Y. Gao, and L. Hanzo, "Enhancing the physical layer security of non-orthogonal multiple access in large-scale networks," *IEEE Trans. Wireless Commun.*, vol. 16, no. 3, pp. 1656–1672, Mar. 2017.

[25] H. Zhang, N. Yang, K. Long, M. Pan, G. K. Karagiannidis, and V. C. M. Leung, "Secure communications in NOMA system: Subcarrier assignment and power allocation," *IEEE J. Sel. Areas Commun.*, vol. 36, no. 7, pp. 1441–1452, Jul. 2018.

[26] Y. Sun, D. W. K. Ng, J. Zhu, and R. Schober, "Robust and secure resource allocation for full-duplex MISO multicarrier NOMA systems," *IEEE Trans. Commun.*, vol. 66, no. 9, pp. 4119–4137, Sep. 2018.

[27] S. Han, X. Xu, X. Tao, and P. Zhang, "Joint power and sub-channel allocation for secure transmission in NOMA-based MMTC networks," *IEEE Syst. J.*, to be published.

[28] L. Liu and W. Yu, "Massive connectivity with massive MIMO—Part I: Device activity detection and channel estimation," *IEEE Trans. Signal Process.*, vol. 66, no. 11, pp. 2933–2946, Jun. 2018.

[29] P. Soldati, "Interference coordination and resource allocation in dense small cell networks," in *Proc. Int. Conf. GLOBECOM*, Austin, TX, USA, Dec. 2014, pp. 3742–3747.

[30] T. Lv, Y. Ma, J. Zeng, and P. T. Mathiopoulos, "Millimeter-wave noma transmission in cellular M2M communications for Internet of Things," *IEEE Internet Things J.*, vol. 5, no. 3, pp. 1989–2000, Jun. 2018.

[31] D. Zhai, R. Zhang, L. Cai, B. Li, and Y. Jiang, "Energy-efficient user scheduling and power allocation for NOMA-based wireless networks with massive IoT devices," *IEEE Internet Things J.*, vol. 5, no. 3, pp. 1857–1868, Jun. 2018.

[32] Y. Sun, D. W. K. Ng, Z. Ding, and R. Schober, "Optimal joint power and subcarrier allocation for full-duplex multicarrier non-orthogonal multiple access systems," *IEEE Trans. Commun.*, vol. 65, no. 3, pp. 1077–1091, Mar. 2017.

[33] S. Tomida and K. Higuchi, "Non-orthogonal access with SIC in cellular downlink for user fairness enhancement," in *Proc. IEEE Int. Symp. Intell. Signal Process. Commun. Syst.*, Chiang Mai, Thailand, Dec. 2011, pp. 1–6.

[34] Y. J. Zhang, L. P. Qian, and J. Huang, "Monotonic optimization in communication and networking systems," *Found. Trends Netw.*, vol. 7, no. 1, pp. 1–75, Oct. 2013.

[35] A. Behnad and X. Wang, "Distance statistics of the communication best neighbor in a Poisson field of nodes," *IEEE Trans. Commun.*, vol. 63, no. 3, pp. 997–1005, Mar. 2015.

[36] M. Haenggi, J. G. Andrews, F. Baccelli, O. Dousse, and M. Franceschetti, "Stochastic geometry and random graphs for the analysis and design of wireless networks," *IEEE J. Sel. Areas Commun.*, vol. 27, no. 2, pp. 1029–1046, Sep. 2009.

[37] X. Gao, A. Behnad, and X. Wang, "Performance analysis of decode-and-forward dual-hop opportunistic relaying with power control," in *Proc. IEEE Int. Conf. Commun.*, Sydney, NSW, Australia, Jun. 2014, pp. 4832–4837.

[38] Z. Ding, P. Fan, and H. V. Poor, "Impact of user pairing on 5G non-orthogonal multiple access downlink transmissions," *IEEE Trans. Veh. Technol.*, vol. 65, no. 8, pp. 6010–6023, Aug. 2016.

[39] L. Lei, D. Yuan, C. K. Ho, and S. Sun, "Joint optimization of power and channel allocation with non-orthogonal multiple access for 5G cellular systems," in *Proc. IEEE GLOBECOM*, San Diego, CA, USA, Dec. 2015, pp. 1–6.

[40] A. Kuhestani, A. Mohammadi, and M. Mohammadi, "Joint relay selection and power allocation in large-scale MIMO systems with untrusted relays and passive eavesdroppers," *IEEE Trans. Inf. Forensics Security*, vol. 13, no. 2, pp. 341–355, Feb. 2018.

[41] A. Kuhestani, A. Mohammadi, K.-K. Wong, P. L. Yeoh, M. Moradikia, and M. R. A. Khandaker, "Optimal power allocation by imperfect hardware analysis in untrusted relaying networks," *IEEE Trans. Wireless Commun.*, vol. 17, no. 7, pp. 4302–4314, Jul. 2018.

[42] J. Huang and A. L. Swindlehurst, "Robust secure transmission in MISO channels based on worst-case optimization," *IEEE Trans. Signal Process.*, vol. 60, no. 4, pp. 1696–1707, Apr. 2012.

[43] M. R. Abedi, N. Mokari, H. Saeedi, and H. Yanikomeroglu, "Robust resource allocation to enhance physical layer security in systems with full-duplex receivers: Active adversary," *IEEE Trans. Wireless Commun.*, vol. 16, no. 2, pp. 885–899, Feb. 2017.

[44] T. Wang and L. Vandendorpe, "Iterative resource allocation for maximizing weighted sum min-rate in downlink cellular OFDMA systems," *IEEE Trans. Signal Process.*, vol. 59, no. 1, pp. 223–234, Jan. 2011.

[45] K. Son, S. Lee, Y. Yi, and S. Chong, "REFIM: A practical interference management in heterogeneous wireless access networks," *IEEE J. Sel. Areas Commun.*, vol. 29, no. 6, pp. 1260–1272, Jun. 2011.

[46] N. Mokari, F. Alavi, S. Parsaeefard, and T. Le-Ngoc, "Limited-feedback resource allocation in heterogeneous cellular networks," *IEEE Trans. Veh. Technol.*, vol. 65, no. 4, pp. 2509–2521, Apr. 2016.

[47] D. T. Ngo, S. Khakurel, and T. Le-Ngoc, "Joint subchannel assignment and power allocation for OFDMA femtocell networks," *IEEE Trans. Wireless Commun.*, vol. 13, no. 1, pp. 342–355, Jan. 2014.

[48] *NOMAD Solver*. Accessed: 2017. [Online]. Available: http://www.i2c2.aut.ac.nz/Wiki/OPTI/index.php/Solvers/NOMAD

[49] CVX Research. (Aug. 2012). *CVX: MATLAB Software for Disciplined Convex Programming, Version 2.0*. [Online]. Available: http://cvxr.com/cvx

[50] L. Venturino, N. Prasad, and X. Wang, "Coordinated scheduling and power allocation in downlink multicell OFDMA networks," *IEEE Trans. Veh. Technol.*, vol. 58, no. 6, pp. 2835–2848, Jun. 2009.

[51] S. Boyd, and L. Vandenberghe, *Convex Optimization*. Cambridge, U.K.: Cambridge Univ. Press, 2004.
[52] J. Zhao, Y. Liu, K. K. Chai, A. Nallanathan, Y. Chen, and Z. Han, "Resource allocation for non-orthogonal multiple access in heterogeneous networks," in *Proc. IEEE Int. Conf. Commun.*, Paris, France, May 2017, pp. 1–6.
[53] H. H. Kha, H. D. Tuan, and H. H. Nguyen, "Fast global optimal power allocation in wireless networks by local D.C. Programming," *IEEE Trans. Wireless Commun.*, vol. 11, no. 2, pp. 510–515, Feb. 2012.
[54] A. Zappone, E. Björnson, L. Sanguinetti, and E. Jorswieck, "A framework for globally optimal energy-efficient resource allocation in wireless networks," in *Proc. IEEE Int. Conf. Acoust. Speech Signal Process.*, Shanghai, China, Mar. 2016, pp. 3616–3620.
[55] A. Zappone, E. Björnson, L. Sanguinetti, and E. Jorswieck, "Globally optimal energy-efficient power control and receiver design in wireless networks," *IEEE Trans. Signal Process.*, vol. 65, no. 11, pp. 2844–2859, Jun. 2017.

MOSLEM FOROUZESH received the M.Sc. degree in electrical engineering from Tarbiat Modares University, Tehran, Iran, in 2015, where he is currently pursuing the Ph.D. degree with the Department of Electrical Engineering. His current research interests include non-orthogonal multiple access (NOMA), radio resource allocation in wireless networks, physical layer security, and covert communication.

PAEIZ AZMI was born in Tehran, Iran, in April 1974. He received the B.Sc., M.Sc., and Ph.D. degrees in electrical engineering from the Sharif University of Technology (SUT), Tehran, in 1996, 1998, and 2002, respectively.

From 1999 to 2001, he was with the Advanced Communication Science Research Laboratory, Iran Telecommunication Research Center (ITRC), Tehran, where he was with the Signal Processing Research Group, from 2002 to 2005. Since September 2002, he has been with the Electrical and Computer Engineering Department, Tarbiat Modares University, Tehran, where he became an Associate Professor, in January 2006, and is currently a Full Professor. His current research interests include modulation and coding techniques, digital signal processing, wireless communications, radio resource allocation, molecular communications, and estimation and detection theories.

NADER MOKARI received the Ph.D. degree in electrical engineering from Tarbiat Modares University, Tehran, Iran, in 2014, where he joined the Department of Electrical and Computer Engineering, as an Assistant Professor, in 2015. He has been involved in a number of large scale network design and consulting projects in the telecom industry. His research interests include design, analysis, and optimization of communication networks.

KAI-KIT WONG received the B.Eng., M.Phil., and Ph.D. degrees in electrical and electronic engineering from The Hong Kong University of Science and Technology, Hong Kong, in 1996, 1998, and 2001, respectively. He held academic and research positions at The University of Hong Kong, Lucent Technologies, Bell-Labs, Holmdel, the Smart Antennas Research Group, Stanford University, and the University of Hull, U.K. He is currently the Chair of wireless communications with the Department of Electronic and Electrical Engineering, University College London, U.K. His current research interests include around 5G and beyond mobile communications, including topics such as massive multiple-input multiple-output, full-duplex communications, millimeter-wave communications, edge caching and fog networking, physical layer security, wireless power transfer, and mobile computing

HOSSEIN PISHRO-NIK received the B.S. degree from the Sharif University of Technology, and the M.Sc. and Ph.D. degrees from the Georgia Institute of Technology, all in electrical and computer engineering. He is currently an Associate Professor of electrical and computer engineering with the University of Massachusetts, Amherst, MA, USA. He was a recipient of the NSF Faculty Early Career Development (CAREER) Award, the Outstanding Junior Faculty Award from UMass, and the Outstanding Graduate Research Award from the Georgia Institute of Technology.